RIPENESS	SENSOR	DEVEL	OPMENT
Final Repo	ort		

November 1992

Work Performed Under Contract No. FC02-89ID12917

For U.S. Department of Energy Pittsburgh Energy Technology Center Pittsburgh, Pennsylvania By

Purdue University
West Lafayette, Indiana

DISCLAIMER

This report was prepared as an account of work sponsored by an agency of the United States Government. Neither the United States Government nor any agency thereof, nor any of their employees, makes any warranty, express or implied, or assumes any legal liability or responsibility for the accuracy, completeness, or usefulness of any information, apparatus, product, or process disclosed, or represents that its use would not infringe privately owned rights. Reference herein to any specific commercial product, process, or service by trade name, trademark, manufacturer, or otherwise does not necessarily constitute or imply its endorsement, recommendation, or favoring by the United States Government or any agency thereof. The views and opinions of authors expressed herein do not necessarily state or reflect those of the United States Government or any agency thereof.

This report has been reproduced directly from the best available copy.

Available to DO's and DOE contractors from the Office of Scientific and Technical Information, P.O. Box 62, Oak Ridge, TN 37831; prices available from (615)576-8401.

Available to the public from the National Technical Information Service, U. S. Department of Commerce, 5285 Port Royal Rd., Springfield, VA 22161.

RIPENESS SENSOR DEVELOPMENT

Final Report

November 1992

Work Performed Under Contract No. DE-FC07-89ID12917

Prepared for the
U.S. Department of Energy
Under DOE Idaho Field Office
Sponsored by the Office of the Assistant Secretary
for Conservation and Renewable Energy
Office of Industrial Technologies
Washington, D.C.

Prepared by
Department of Agricultural Engineering
Purdue University
West Lafayette, IN 47907

TABLE OF CONTENTS

	Pa	ge
ΕZ	CUTIVE SUMMARY	1
B	KGROUND	2
	eferences	3
	ables	4
1.	STIMATE OF ENERGY SAVINGS	5
	1 Invested Energy	5
	2 Utilized Energy	6 7
	eferences	7
	igures	8
2.	EASIBILITY STUDIES ON SUGAR CONTENT MEASUREMENTS	9
	1 Materials and Methods	9
	2 Water-Sugar Solutions	9
		10 10
	eferences	10
	eferences	12
3.	EVIEW ON WATER PEAK SUPPRESSION TECHNIQUES	15
	1 Excitation and Irradiation Techniques	15
		16
		16 16
		17
	eferences	17
		19
4.		20
		20
	 	20 21
		21
	5 Inversion Recovery Sequence	21
	o building or biginious a manage of the control of	22
	eferences	22

	P	age
	Figures	24
5.	NON-DESTRUCTIVE TESTS ON INTACT FRUIT	27
	5.1 Chemical Exchange and Correlation Model	27
	5.2 Experimental Evidence for the Correlation	28 29
	References	29
	Figures	31
6.	RIPENESS SENSOR DEVELOPMENT: PROTOTYPE	32
	6.1 Magnetic Console Design	32
	6.2 Probe Design	33 33
	6.3 RF Transmitter Circuits	34
	6.5 Computer and Data Acquisition Board	34
	References	34
	Figures	36
7.	PRELIMINARY TESTS USING THE PROTOTYPE	38
	7.1 Analysis of the Signal	38
	7.2 Test of Sugar Solutions	39
	7.3 Test of Intact Fruit	39
	7.4 Conclusions	40 40
	References	40
	Figures	41
SI	MMARY	46
R	COMMENDATIONS	50

LIST OF TABLES

Table						Pa	age
Carbohydrates and Sugars in Selected Raw Fruit and Vegetable		•		•	•		4

LIST OF FIGURES

Figur	e					F	Page
1. C	Concept of the utilized energy saving			•	•		8
2. E	Block diagram of a typical ¹ H-MR spectrometer			•			12
3. T	The ¹ H-MR spectrum of 10% sugar-water mixture			•		•	13
4. C	Correlation of sugar content to the highest sugar peak from sugar-water mixtures		, c	•			13
5. T	The ¹ H-MR spectrum of a well-ripened banana sample						13
6. C	Correlation between ripeness of bananas and height of sugar peak					•	14
7. C	Correlation between ripeness apples and height of sugar peak		, ,		•		14
8. S	Some criteria for choosing a good water peak suppression method			•			19
	Correlation between hydrogen T_1 (of water and sugar resonances) and refractomet neasurements of sugar content in muskmelon	ter				•	24
	Correlation between ¹ H-MR sugar peak height and sugar content in muskmelon usingle pulse technique	ısin;	g th	1e		•	25
	Correlation between ¹ H-MR sugar peak height and sugar content in muskmelon the IRFT pulse technique	issu •	ie u	ısin •	g •	•	26
	Correlation between sugar content (measured with a refractometer) and T_2 relaxat ntact individual 'Red Flame' seedless grapes	ion	. tin	nes •	fo	r •	31
	Correlation between sugar content (measured with a refractometer) and T_2 relaxat ntact Washington sweet cherries	ion	tin	nes	fo	r •	31
14. \$	Schematic diagram of the prototype ripeness sensor	•	•		•		36
15. 7	The magnet console configuration of the ¹ H-MR based sensor	•	•			•	36
16. C	Circuit diagram for the prototype ripeness sensor	•	•	•	•		37
17. (Output signals from glycerin and water samples		•	•			41
	Output signals from different sugar solution samples. The phase of the resonance shifted by -180° compared to the signals in Figure 17	sigi •	nals •	s is •	•	•	42
	Output signals from individual grapes. The phase of the resonance signals is shiften to the signals in Figure 17.						43

	Figure	Page
	20. Output signal from green and yellow bananas. The phase of the resonance signals is shifted by -180° compared to the signals in Figure 17	44
•	21. Output signal from individual grapes. The phase of the resonance signals is shifted by -180° compared to the signals in Figure 17	45
•		

е .

EXECUTIVE SUMMARY

Sensor development for quality control is a critical part of today's food handling system. Use of a non-destructive ripeness sensor for monitoring ripeness of fruit and vegetables from production to distribution can help maintain the value of a product, save substantial *invested* and *utilized* energy, and improve consumer satisfaction.

About 20 - 25% of the total production of fruits and vegetables in the USA must be discarded after harvest. About 25 - 30% of this loss is the result of over-ripening and this loss represents about 8.39×10^{12} BTU of *invested energy* every year. This *invested energy* could be saved by non-destructive ripeness sensing. According to our calculation the energy *utilized* for storage, distribution and transportation could be also reduced by 17 - 38%. Therefore, about **0.0242 quad** (i.e. 24.2×10^{12} BTU) of total energy could be saved each year.

Sweetness is an important indicator of fruit quality and highly correlated with ripeness in most fruits. Riper fruits have higher sugar contents. Since 1987, research to develop a non-destructive fruit ripeness sensor has been conducted in the Agricultural Engineering Department at Purdue University. It is based on ¹H-MR (proton Magnetic Resonance). The Department of Energy (DOE) supported a research project (Phase I) which developed a prototype ripeness sensor and included feasibility studies.

A first generation prototype of the ripeness sensor (based on ¹H-MR) was built and tested with intact small fruit (such as grapes). Results show that the sensor can discriminate small fruit (0.75 in diameter or smaller) differing in sugar content by 6% (or more). This prototype can separate the fruit into at least two groups: one *ripe* and the other *not ripe*. The estimated cost for such a ripeness sensor is around \$4,000.

The signal sensitivity of the prototype can be improved to enable it to differentiate between fruits varying in sugar content by only 1 or 2%. This can be achieved by: (a) using water peak suppression techniques to recover relatively weak sugar resonance signals in intact fruits, (b) modifying circuits to eliminate noise, leakage and distortion of input/output signals, (c) improving the magnetic console to get a higher magnetic field and better homogeneity, and (d) designing a probe to achieve a higher signal-to-noise (S/N) ratio. As research continues a second generation ripeness sensor will be developed which will incorporate many of the improvements and which will be suitable for commercial use. Additional research will allow application of the technique to a wider range of fruit sizes (from blueberries to watermelons). It would provide considerable energy savings and improve fruit quality. Therefore, it could have a significant economic impact on the fresh food market.

This report describes (1) estimated energy savings, (2) feasibility studies, (3) development of the initial prototype, and (4) preliminary evaluation of the *first generation* prototype.

BACKGROUND

More than 80 kinds of fruits and vegetables are available in the United States. But only about 6 of them have quality standards (Dull, 1986). Consumers want quality fruit that looks and tastes good. In a 1990 survey (Zind, 1990), consumers rated 16 characteristics important in their decision when purchasing fresh produce. The most important factors were ripeness/freshness, taste/flavor, appearance/condition and nutritional value. Of those surveyed, 96% rated ripeness/freshness as extremely important, or very important.

Nondestructive quality control in fruits and vegetables is a goal of growers, distributors, and food processors. Determining a fruit's quality is difficult unless it is cut and tasted. Good taste is based on sugar and acid content, and flavor. In most fruits, taste highly correlates with soluble solids content, which is largely sugars. Thus, nondestructive evaluation of soluble solids (or sugar content) should indicate fruit quality.

Conventionally fruits are determined to be ready for harvest by a destructive chemical laboratory analysis of random samples, or by tasting for flavor and observing physical factors such as color, texture, firmness, shape, lack of defects, etc. Several nondestructive techniques have been developed to grade or sort raw fruit, including the following techniques: machine vision, soft X-rays, ultrasonics, optical transmission and infrared radiation. However, these grading methods are not totally reliable and the individual fruit may not be graded properly because cultural practices, soil moisture and temperature often affect physical observations (such as color) more than does physiological maturity.

Sugar content is one of the best indications of fruit quality and is highly related to ripeness in most fruits and some vegetables. The compositions of several fresh fruits and vegetables are shown in Table 1 (Ensminger et al., 1983). The average sugar content of ripe fruits varies from approximately 5% to 20% while the water content ranges from 80% to 90%. However, the sugar content increases as the fruit ripens. For example, the sugar content of sweet cherries may vary from 10% to 23%. The optimum range for harvest is considered to be 14% to 16%. Some fruits, such as apples, apricore, bananas, peaches and pears are climacteric and they can ripen during storage after harvest. During ripening sugar content increases. For example, a green banana may contain 8% sugar while a very ripe banana contains 20% sugar.

There are few reports of successful nondestructive measurements of sugar content directly in fruit. Sugar content in thin-skinned fruits such as peaches has been measured with near infrared radiation (Bellon et al., 1989; Dull, 1986), but the correlation was low (correlation coefficient r=0.6) in thick-skinned fruits such as melons (Dull et al., 1989). Sugar content is measured only near the skin, and the skin of fruits can be damaged during the measurement.

Higher quality fruit could be harvested and made available to consumers if there were a non-destructive and non-contact sensor that detects ripeness level directly by measuring sugar content in the entire single fruit. Only the proton (¹H) Magnetic Resonance (¹H-MR) principle is promising for this type of sensing. It provides electrical signals proportional not only to the total concentration of selected nuclei (or protons), but also to the amounts of particular components or molecules in the sample being measured.

Ripeness Sensor Dev. Background

Section 1 of this report summarizes the potential for energy savings from use of the ripeness sensor. Sections 2 through 5 report the results of feasibility studies on the ripeness sensor. Sections 6 and 7 describe the prototype and the results of preliminary tests with the prototype.

References

- [1] Bellon, V., and Boisde, G. 1989. Remote Near Infrared Spectroscopy in Food Industry with the use of silica and fluoride glasses fibers. pg. 350-359 in: Proceedings of the conference SPIE. January 17-19, 1989, Los Angeles, CA.
- [2] Belton, P.S., Colquhoun, I.J. 1989. Nuclear Magnetic Resonance Spectroscopy in Food Research. Spectroscopy 4(2): 22-32
- [3] Cho, S.I. 1989. Development of a Nuclear Magnetic Resonance Based Sensor Development to Detect Ripeness of Fruit. Unpublished Ph.D. dissertation, Agricultural Engineering, Purdue University, West Lafayette, IN.
- [4] Dull, G.G. 1986. Nondestructive evaluation of quality of stored fruits and vegetables. Food Technol. 40(5):106-110.
- [5] Dull, G.G., Birth, G.S., Smittle, D.A., Leffler, R.G. 1989. Near Infrared Analysis of Soluble Solids in Intact Cantaloupe. J. Food Sci. 54(2):393-395.
- [6] Ensminger, E.S., M.E. Ensminger, J.E. Konlaude and J.R.K. Robson. 1983. Food & Nutrition Encyclopedia. Vol 1 and 2. Pegus Press, Clovis, CA.
- [7] Gadian, D.G. 1982. Nuclear Magnetic Resonance and its Application to Living Systems. Clarendon Press, Oxford, UK.
- [8] Zind, T. 1990. Fresh Trends '90, A profile of Fresh Produce Consumers. The Packer 97:37-66.

Tables

Table 1. Carbohydrates and Sugars in Selected Raw Fruit and Vegetable

		Water*	Carbohydrates	Sugar#	Fiber
Fruits	Apricots	85.3	12.8	6.1	0.6
	Banana	75.7	22.2	19.6	0.5
	Blackberries	84.5	12.9	7.0	0.5
	Cantaloupe	91.2	7.5	6.5	0.3
	Sweet Cherries	80.4	17.4	14.1	0.4
	Grapes	81.6	17.3	16.9	0.6
	Grapefruit	88.4	10.6	5.2	0.2
	Honeydew	90.6	7.7	4.1	0.6
	Mango	81.7	16.8	7.4	0.9
	Orange	36.0	12.2	8.5	0.5
}	Peach	89.1	9.7	8.5	0.6
	Pear	83.2	15.3	8.7	1.4
	Pineapple	85.3	13.7	10.6	0.4
	Plums	86.8	11.9	5.4	0.3
	Strawberres	89.9	8.4	4.5	1.3
	Watermelon	92.6	6.4	3.2	0.6
Vegetables	Carrots	88.2	9.7	5.9	1.0
	Onions	89.1	8.7	7.9	0.6
	Peas	78.0	14.4	5.5	2.0
	Tomatoes	93.5	4.7	2.8	0.5
	Sweet Potatoes	63.7	32.5	7.2	0.9

^{*}Portion of a 100 gram sample. Data was referred to the HVH-CWRU Nutrient Data Base developed by the Division of Nutrition, Highland View Hospital, and department of Biometry and Nutrition, School of Medicine, Case Western Reserve University, Cleveland, Ohio.

[#]Average sugar content. The sugar content of ripe fruit and vegetables may be higher.

1. ESTIMATE OF ENERGY SAVINGS

Energy conservation is an important issue in both industry and agriculture. The US is largely dependent on foreign energy sources such as oil. About 23% of the total fresh food (fruits and vegetables) production is lost every year in the US. This wasted energy should be saved. According to our survey, a significant amount of energy is also wasted during storage, distribution, and transportation of harvested fruits and vegetables. Also, local distributors told us that about 15% of their fresh produce is lost before it can be sold. They said that they could decrease the loss to 5% if a sensor which could monitor ripeness of fruits and vegetables were available. The energy which we describe here as *invested energy* is the energy used in growing the fruits and vegetables. *Utilized energy* is the energy used to bring them to market.

1.1 Invested Energy

The following is a detailed description of the estimate of the invested energy which could be saved by utilizing a ripeness sensor. A total of thirteen fruits were considered in this calculation: apples, apricots, avocados, bananas, cherries, grapes, grapefruit, oranges, papayas, peachs, pears, pineapples, and strawberries. The following four vegetables were also considered: cantaloupe, honeydew, tomatoes, and watermelon.

According to the USDA (Agricultural Statistics, 1988) the total U.S. production of the thirteen fruits was 28.3 million tons in 1988. The total production for the four vegetables was 11.1 million tons. The average energy cost for producing the fruits was 3.44×10^6 BTU/ton while the cost for the vegetables was 2.48×10^6 BTU/ton (R.C. Fluck et al., Agricultural Energetics, 1980). Average losses after harvest were about 22.9 % for the thirteen fruits and 22.8 % for the four vegetables.

Assuming 20 to 30% of the losses (due to spoilage caused by the lack of ripeness monitoring) could be prevented if the ripeness sensor were used, the estimated energy savings would be:

(1) For a 20% recovery rate

Fruit:

[28.3 million tons] \times [3.44 · 10⁶ BTU/ton] \times 0.229 \times 0.2 = 4.459 \times 10¹² BTU

Vegetables:

11.1 [million tons] $\times 2.48 \cdot 10^6$ [BTU/ton] $\times 0.228 \times 0.2 = 1.255 \times 10^{12}$ BTU

TOTAL: 5.7×10^{12} BTU per year.

(2) For a 30% recovery rate:

Ripeness Sensor Dev. Estimate of Energy

Fruit:

 $[28.3 \text{ million tons}] \times [3.44 \cdot 10^6 \text{ BTU/ton}] \times 0.229 \times 0.3 = 6.688 \times 10^{12} \text{ BTU}$

Vegetables:

[11.1 million tons] \times [2.48 · 10⁶ BTU/ton] \times 0.228 \times 0.3 = 1.883 \times 10¹² BTU

TOTAL: 8.6×10^{12} BTU per year.

During the spring of 1990, we conducted a literature search and contacted people working in the fruit and vegetable industry in order to determine the average losses which occur in the handling and marketing of fruits and vegetables. Included in our phone contacts were USDA scientists, grocery store managers, and produce wholesalers. On the basis of this information, the approximate recoverable losses were 31.5% for the fruit and 21.9% for the vegetables. Using these figures, the energy savings for the selected fruits would be approximately 7.02×10^{12} BTU and the energy savings for the selected vegetables would be approximately 1.37×10^{12} BTU. This gives a total yearly energy savings of 8.39×10^{12} BTU. This is equivalent to a yearly savings of about 60 million gallons of gasoline or about 9,000 million cubic ft of natural gas.

1.2 Utilized Energy

Additional energy savings are possible during storage, transportation, and distribution of the harvested fruits (28.3 million tons) and vegetables (11.1 million tons). Assuming that 1500 BTU/ton (at 40° F) is used each day for cooling and that cooling is needed 200 days a year, the energy needed for cooling during storage and distribution is 12×10^{12} BTU/year. If 80% of the fresh produce is transported by truck, another 20×10^{12} BTU/year is needed for transportation. Therefore, the total utilized energy for storage, transportation and distribution amounts to 32×10^{12} BTU a year. If imported fruits and vegetables are counted, the total energy consumption would be approximately twice this value, 64×10^{12} BTU, each year. The following example illustrates the procedure for calculating energy savings.

Harvested fruits are routinely stored in cooling facilities for several weeks or more while they further ripen naturally. For example, at the time of harvest, 60 boxes of apples could be separated into four groups according to their ripeness (or sweetness) using the ripeness sensor: (A) well-ripened apples ready to ship, (B) ripe apples which can be stored for a week, (C) moderately ripened apples which need to be stored for two weeks, and (D) slightly ripened apples which can be stored for three weeks or be used for apple pie or sauce. The following estimates are based on the assumption that the energy consumption for a cooler is 700 BTU/box/day.

With the Ripeness Sensor

In this scenario, the sensor is used to sort the harvested apples according to sugar content: 10 boxes in group (A), 20 boxes in group (B), 20 boxes in group (C), and 10 boxes in group (D). Each group is stored in separate coolers (I, II, III, IV in Figure 1). The apples in group (A) have a high sugar content and are ready to ship so that no storage is necessary. The apples in group (B) have a medium sugar content and are stored for one week. The apples in group (C) have a relatively low sugar content and are stored for two weeks so that sugar content increases as a result of ripening during storage. The apples in group (D) have a low sugar content and require storage for three weeks. Half of them can be processed for apple juice or sauce with no storage. Therefore, the total utilized energy consumption is:

 $(20 [boxes] \times 700 [BTU/box/day] \times 7 days) + (20 [boxes] \times 700 [BTU/day] \times 14 days) + (5 boxes \times 700 [BTU/box/day] \times 21 days) = 367,500 BTU.$

Without the Ripeness Sensor

In this second scenario, the harvested apples are not sorted according to their ripeness or sweetness. The 60 boxes of ungraded apples are stored in three coolers for two weeks (or 20 boxes each in I, II, and III in Figure 1). The energy consumption is: 3×20 [boxes] $\times 700$ [BTU/box/day] $\times 14$ days = 588,000 BTU. The total energy consumption with the sensor is about 37.5% higher than the consumption with the sensor. This suggests that about 9×10^{12} BTU (i.e. $0.375 \times 24 \times 10^{12}$ BTU) can be saved during storage and distribution. About 17% or more (10 boxes in **group** (A) + some of in **group** (B)) would be over-ripe when removed from the coolers and could easily spoil during transportation or distribution. In other words, at least 17% of the energy for transportation could be saved. This is equivalent to 6.8×10^{12} BTU (i.e. $0.17 \times 40 \times 10^{12}$ BTU) a year.

1.3 Conclusion

Ripeness sensing can save a significant amount of energy (both *invested* and *utilized energy*) and at the same time improve quality control for the fresh food market. The ripeness sensor can non-destructively monitor ripeness thereby preventing much of the loss due to over-ripening. By sorting fruit and vegetables according to their sugar contents, the sensor can save about 37.5% of the energy utilized for storage and distribution and at least 17% of the energy utilized for transportation. Therefore, the total yearly energy savings amounts to 24.2×10^{12} BTU (i.e. **0.0242 quad**). The total includes 8.39×10^{12} BTU savings for the invested energy, 6.8×10^{12} BTU savings for the energy utilized in storage and distribution. This is equivalent to a yearly savings of approximately **173 million gallons of gasoline**. In addition, over-ripe fruit could be processed into fruit sauce or juice without storage. This would also contribute to the energy savings. There would also be other energy savings which are not included because they are difficult to estimate. For example, the consumer would have to throw away fewer fruits and vegetables due to over-ripening.

References

- [1] Autio, W.R, W.J. Bramlage and W.J. Lord. 1990. Ripening and storability of Marshall McIntosh apples. Fruit Varieties Journal 44:36-40.
- [2] Bolin, H.R., and C.C. Huxsoll. 1989. Storage stability of minimally processed fruit. J. of Food Processing and Preservation, 13:281-292.
- [3] California Agricultural Statistics Service. 1988. California fruit and nut statistics. Sacramento, CA.
- [4] Coursey, D.G. and F.J. Proctor. 1975. Towards the quantification of post-harvest loss in horticultural produce. Acta Hortic., 49:55-66.
- [5] Fluck, R.C. and C.D. Baird. 1980. Agricultural Energetics. AVI Publishing Co., Westport, Conn.
- [6] FAO. 1985. Prevention of post-harvest food losses. Food and Agriculture Organization of the United Nations, Rome.
- [7] Kader, A.A. and J.F. Thompson. 1985. Postharvest Technology of Horticultural Crops. Cooperative Extension, University of California, Division of Agricultural and Natural Resources,

Berkelry, CA.

- [8] Pimentel, D and C.W. Hall. 1984. Food and Energy Resources. Academic Press, New York.
- [9] Ryall, A.L., W.J. Lipton, and W.T. Pentzer. 1979. Handling, transportation and storage of fruits and vegetables. 2nd Edition. AVI Publishing Co., Westport, Conn.
- [10] Salunkhe, D.K. and B.B. Desai. 1984. Postharvest Biotechnology of Fruits. CRC Press, Boca Raton, Fla.
- [11] Sylvia M. Blankenship. 1985. Controlled atmospheres for storage and transport of perishable agricultural commodities. Proceedings of the Fourth National Controlled Atmosphere Research Conferences, July 23-26, 1985 at Raleigh, NC.
- [12] USDA. Agricultural Statistics Summary. 1988. U.S. Government Printing Office, Washington, D.C.

Figures

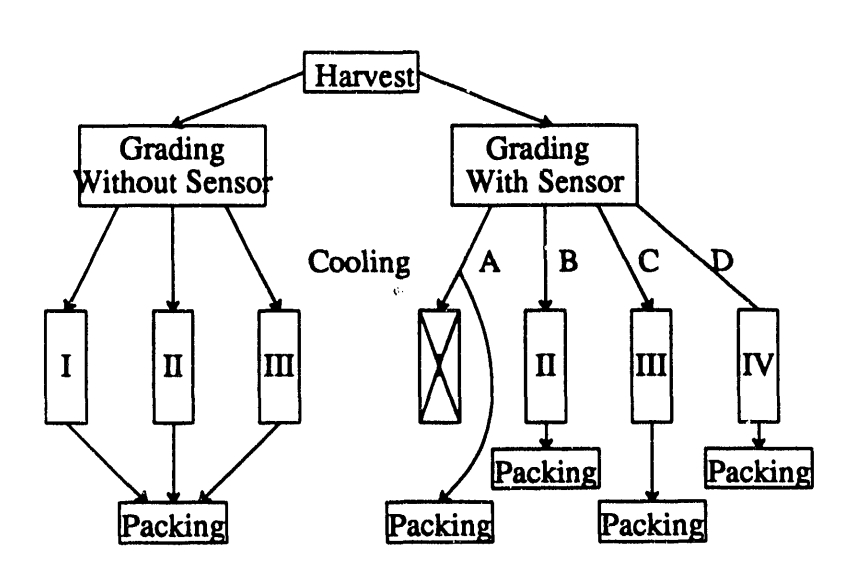


Figure 1. Concept of the utilized energy saving

2. FEASIBILITY STUDIES ON SUGAR CONTENT MEASUREMENTS

¹H-MR is based on the resonant absorption and emission of very low magnetic energy by a proton nucleus subjected to two perpendicular magnetic fields (Figure 2). ¹H-MR spectroscopy is recognized as one of the most powerful techniques for chemical analysis. It can be used to develop sensors which give electrical signals proportional not only to the total concentration of selected nuclei (such as hydrogen nuclei associated with sugars), but also to the amounts of particular components or molecules in the sample. Because it is non-destructive and noncontacting (or non-toxic), ¹H-MR has many potential applications in biological, agricultural and food engineering. The main objective of this study was to investigate the feasibility of using it to detect ripeness of raw fruit.

2.1 Materials and Methods

A 200 MHz high resolution ¹H-MR was used to test water-sugar solutions and fruit cores of bananas and apples. The diameter of the sample was limited to 5 mm. The single pulse technique was employed to detect water and sugar peaks.

The magnetized nuclei induce an electrical signal in an adjacent receiver coil. This is called the free induction decay (FID) signal. Eight FID signals of a sugar-water mixture and sixteen FID signals of a fruit sample were accumulated and processed using the Fourier transformation. The water peak was used as a reference and it was assumed that it had a chemical shift of 4.608 ppm.

The strength of an ¹H-MR signal, which is related to the area under the ¹H-MR spectrum line, is proportional to the number of nuclei contributing to the spectrum line. Sugar peak intensity is proportional to the sugar concentration or total number of sugar molecules. The intensity is represented as the area under the sugar peak. The area under the peak at 3.5±0.25 ppm was used as an indicator of the sugar peak intensity. To calculate the approximate area, we measured sugar peak height from the base line and multiplied it by the average peak width, which we assumed was always constant at 0.5 ppm. This allowed us to simplify our data analysis by using the sugar peak height for the correlation with sugar contents in both sugar-water mixtures and raw fruit samples.

The soluble solids content of each sample was measured with an Atago N1 refractometer. It was assumed that sugar content was equal to soluble solids content. Each sample was smashed and, using an IEC Clinical Centrifuge separator, was separated into a liquid phase, called *supernatant*, and a semi-solid phase. The supernatant was applied to the glass surface of the refractometer.

2.2 Water-Sugar Solutions

The ¹H-MR spectra of fruit could be simulated using water-sugar mixtures. Sugar is almost pure sucrose. Six sugar-water mixtures were used to investigate the correlation of sugar content to ¹H-MR spectra. They contained 2%, 4%, 6%, 8%, 10% and 15% sugar by weight.

Figure 3 shows the ¹H-MR spectra of a 10% sugar-water mixture. The sugar peaks of the ¹H-MR spectra appeared around 3 to 4 ppm. Figure 4 shows the correlation of sugar content to amplitude of the

Ripeness Sensor Dev. Feasibility Studies

highest sugar peak. The correlation was the best (correlation coefficient r=0.987) when the highest sugar peak was used (see Figure 3). This method is promising because it is simple and gives a more rapid quantitative measurement of sugar content than determination of the area under the peak.

2.3 Raw Fruit Core Samples

Two different kinds of raw fruits were tested: bananas and apples. The 5 mm diameter ¹H-MR tube was gently pushed into the fruit so that there was minimal destruction of the tissue. The fruit samples were not smashed or ground. Also, the sample was tested as soon as possible (within 5 minutes) to reduce effects of enzymes that break down sugars.

The fruit samples were a solid-and-liquid mixture consisting of water, sugar and other carbohydrates. To increase the signal-to-noise (S/N) ratio of the fruit samples, the scanning time was increased to twice that of the sugar-water mixture. Figure 5 shows water and sugar peaks of a sample of ripened banana. The peaks were broadened because of non-uniformity inside the sample core. The sugar peak was located around 3.5 ppm. A deconvolution technique could be used to get a narrow sugar peak and the exact peak location.

The amplitudes of the sugar peaks corresponding to the sugar content (closely related to ripeness) of banana and apple samples are plotted in Figures 6 and 7. Linear regression analysis gave correlation coefficients, r, of 0.94 and 0.87, respectively. The *standard errors of correlation* (SEC) were 1.53 and 1.37, respectively.

2.4 Conclusions

The measurement of sugar contents of water-sucrose mixtures using ¹H-MR was quite successful. Ripeness level (or sugar content) of fruit samples was linearly correlated to the amplitude of the sugar peaks. This suggests that raw fruits could be graded into several ripeness categories by the measurement of the amplitude of the sugar peaks. No sugar peak was detected from the unripe (green) bananas, because the strong water peak masked the weak sugar peak. Its sugar content measured with the refractometer was approximately 8%. Therefore, if detection of sugar content of fruits over a wide range of sugar contents is desired, a water peak suppression technique must be used.

References

- [1] Cho, Seong In. 1989. Development of a Nuclear Magnetic Resonance Based Sensor to Detect Ripeness of Fruit. Ph.D. Thesis, Agricultural Engineering, Purdue University, West Lafayette, IN 47907.
- [2] Dull G.C. 1986. Nondestructive evaluation of quality of stored fruits and vegetables. Food Technology 40(5):106-110.
- [3] Fukushima, E. and B.W. Roeder. 1981. Experimental Pulse NMR: a Nuts and Bolts Approach. Addition-Wesley Pub. Co., Reading, MA.
- [4] Hart, Harold. 1987. Organic Chemistry. 7th Ed. Houghton Mifflin Co., Boston, MA.
- [5] Lapedes, D.N. 1977. Food, Agriculture & Nutrition. McGraw-Hill Book Co., New York, NY.

Ripeness Sensor Dev. Feasibility Studies

- [6] Lee, Frank A. 1983. Basic Food Chemistry. 2nd Ed. The AVI Publishing Company Co., Westport, Conn.
- [7] Ryall, A.L. and W.J. Lipton. 1983. Handling, Transportation and Storage of Fruits and Vegetables. 2nd ed, Vol. 1, 2 and 3. AVI publishing Co., Westport, Conn.
- [8] Subcommittee on Sensor Research in Agriculture. November 1986. Research Needs in Sensor Technology for Agriculture. Experiment Station Committee on Organization and Policy. ASAE, St. Joseph, MI.

Figures

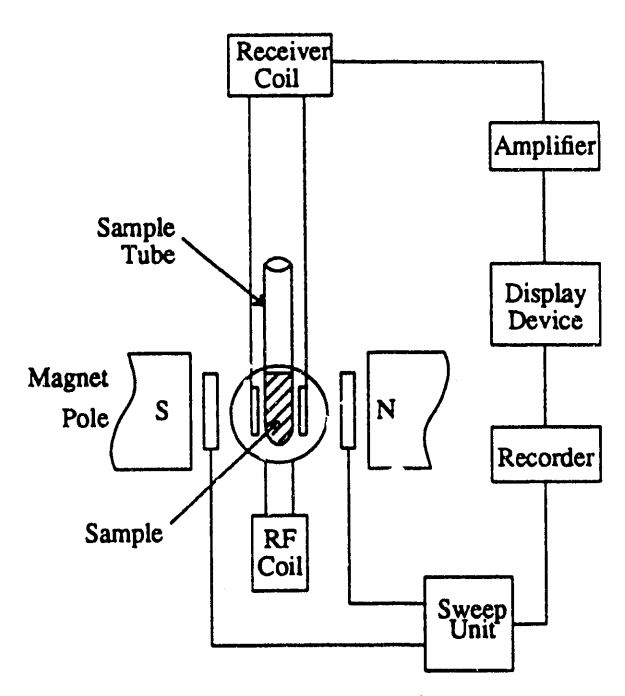


Figure 2. Block diagram of a typical ¹H-MR spectrometer

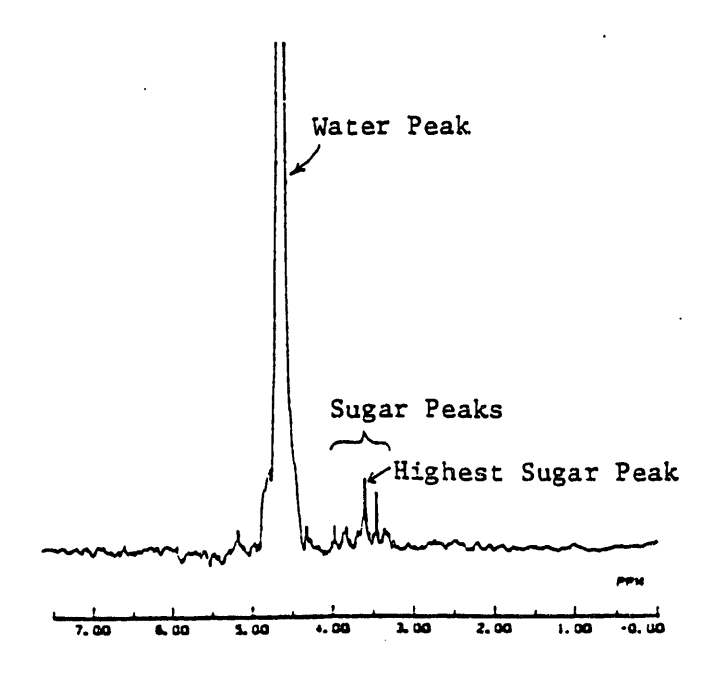


Figure 3. The ¹H-MR spectrum of 10% sugar-water mixture

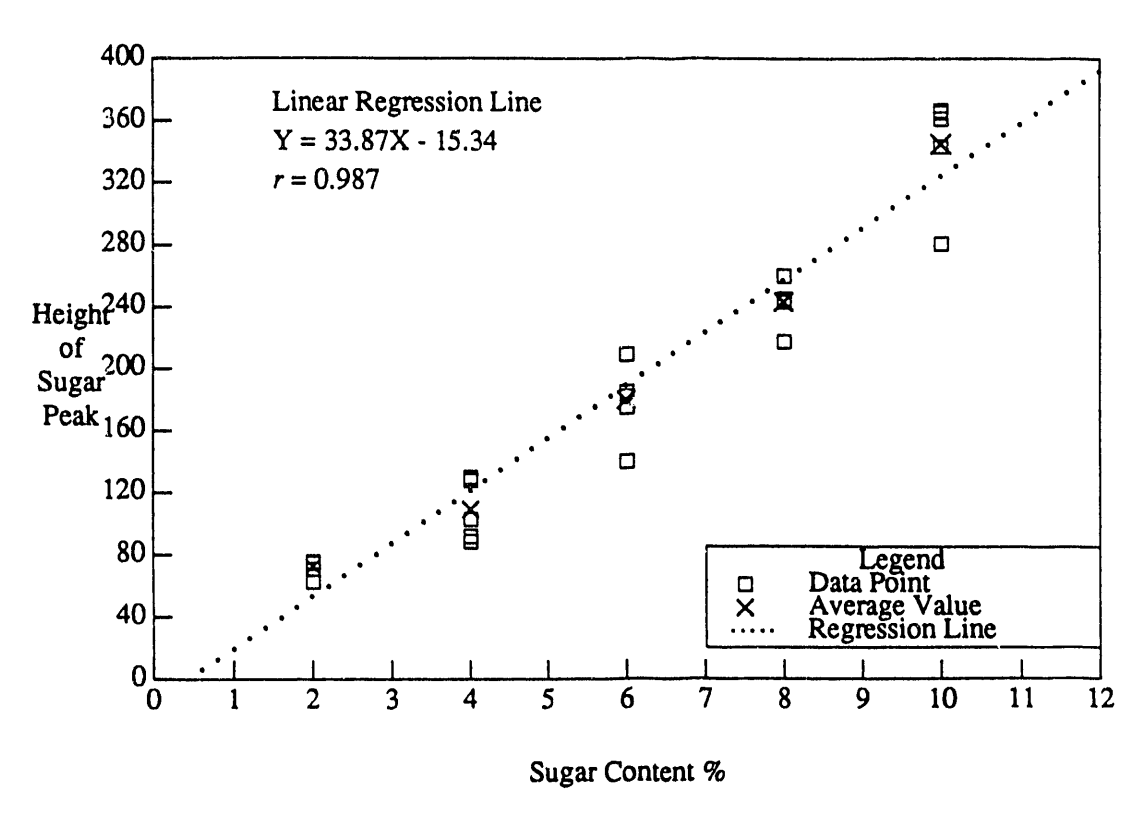


Figure 4. Correlation of sugar content to the highest sugar peak from sugar-water mixtures

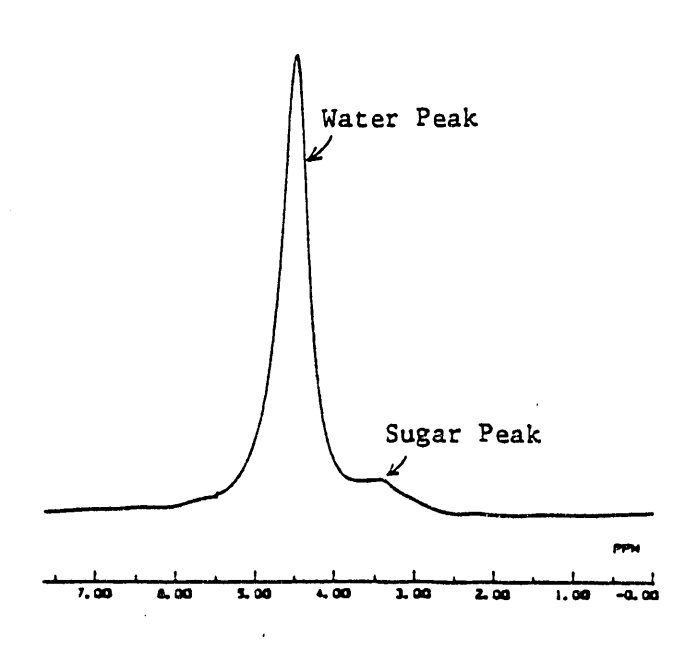


Figure 5. The ¹H-MR spectrum of a well-ripened banana sample

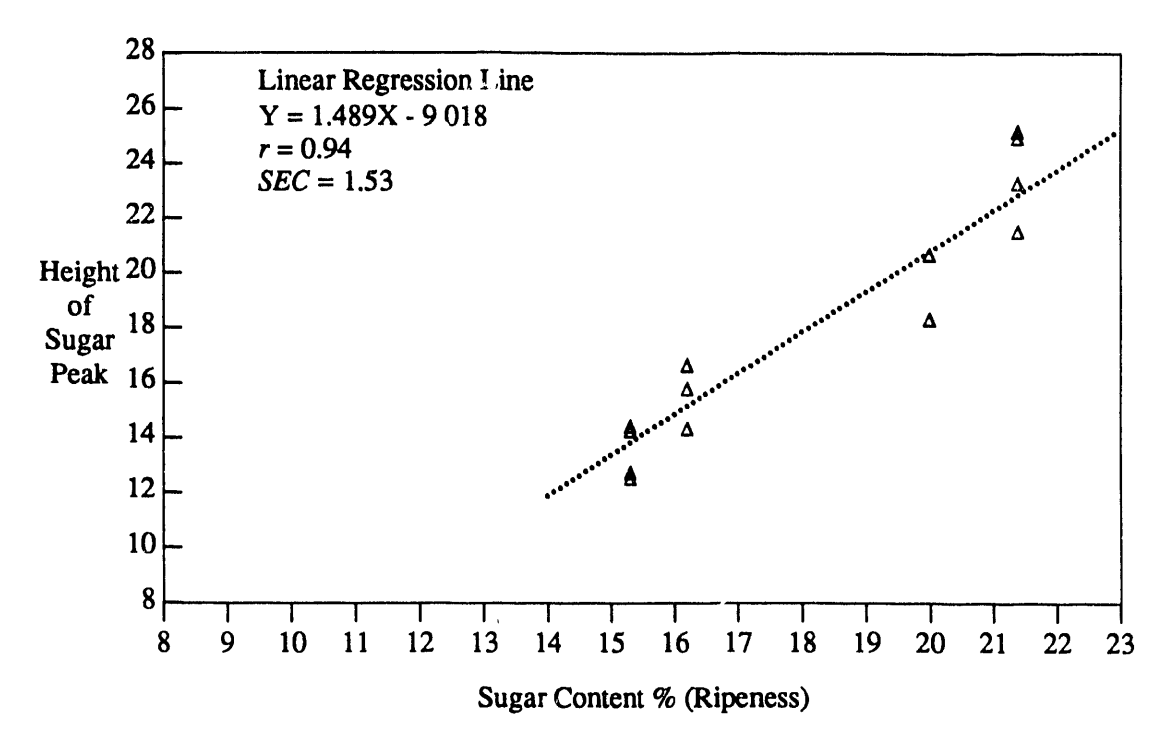


Figure 6. Correlation between ripeness of bananas and height or sugar peak

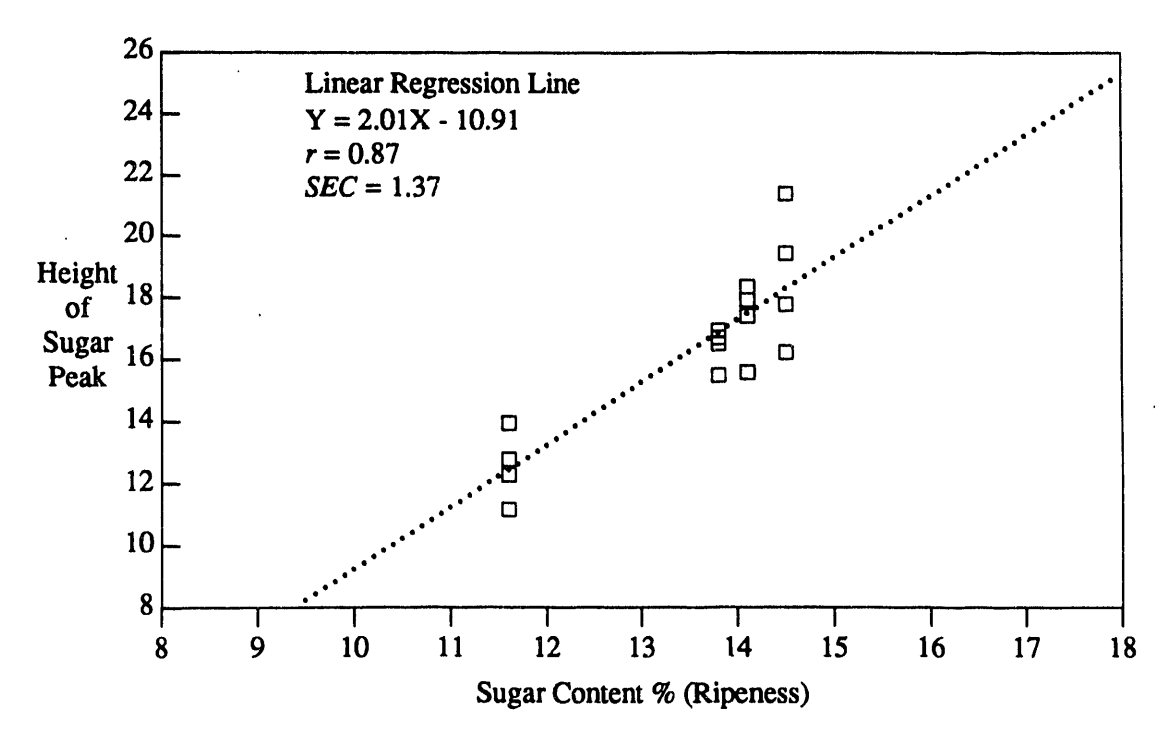


Figure 7. Correlation between ripeness apples and height of sugar peak

3. REVIEW ON WATER PEAK SUPPRESSION TECHNIQUES

Although Fourier transform or pulsed ¹H Nuclear Magnetic Resonance (¹H-MR) spectroscopy has several important advantages over other analytical methods, it is not widely used for the analysis of high water content materials (such as dilute aqueous solutions, and raw fruits and vegetables) because of two major drawbacks: (i) the strong water peak resonance, and (ii) the broad undecipherable aspect of the spectrum due to the ubiquity of the ¹H in biological systems combined with the non selective nature of the ¹H-MR method (strong overlapping background).

As pointed out in the conclusion of part two, in order to study weak metabolite signals (such as those from sugar) in biological systems, the water signal must be suppressed and the resulting spectrum enhanced. As mentioned in the Background section (see Table 1), water content of fresh fruits usually varies from 80% to 95%, and sugar content varies from 5% to 20%. The ¹H-MR spectra of fruit tissue samples contain primarily water and sugar peaks (section 2, Figure 5). The water peak is broad and intense and partially overlaps the sugar peak, making quantification difficult. This problem is worse when inherent resolution of the spectrometer is low, as it is when lower magnetic fields are used. Thus, in developing a fruit ripeness sensor based on ¹H-MR with low magnetic fields, the water resonance should be suppressed. The suppression of a strong peak eliminates the need for excessive demand on receiver linearity and allows the A/D converter to have a narrower dynamic range [10]. This prevents computer memory overflow and rounding errors during the FT operation [6].

Hore [6] classifies the methods of removing the strong solvent signals in two categories: (i) those which try not to excite the intense solvent signal and (ii) those which minimize the solvent magnetization at the time when the resonance frequency is observed. The first category includes selective excitation sequences. Martin et al. [9] proposed two methods which fall in the second category: double irradiation and the use of the differences in relaxation times T_1 between the solute and the solvent. Other researchers [20,2,1,12] have used the T_2 relaxation times to separate a solute with a short- T_2 from a solvent with a longer T_2 .

A question which must be answered for fruit sugar content measurements is which technique should be used for water peak suppression. Two general techniques enable suppression or removal of the water peak. The first technique is selective excitation or irradiation of certain peaks. The second uses the differences between T_1 and T_2 relaxation times. There are many pulse sequences which can be used to accomplish these two general objectives. Detailed reviews on the pulse sequences are given elsewhere [22].

3.1 Excitation and Irradiation Techniques

A major limitation of these techniques occurs when the solute and the solvent peak are close to one another. It is then impossible to irradiate (or excite) one without having an influence on the other. This limitation may be severe in the case of lower field strengths because the resolution is poorer and the bands are closer together.

3.1.a Irradiation Methods

If the solvent peak is wide because of inhomogeneities of the magnetic field B₀, it can not be irradiated by a pulse at the peak frequency. An attempt to do so results in a *burning hole*. Indeed, in this case, the peak is composed of a series of smaller peaks at various frequencies clustered around the center frequency and distributed according to the variation of the magnetic fields in the sample [4]. This makes the FID much shorter and the ¹H-MR line broader.

Generally, when irradiation methods are being used, it is highly recommended that the homogeneity of the magnetic field be improved as much as possible by careful shimming [6]. On the other hand, spatial inhomogeneity of the decoupler is rather a good thing because it increases the dephasing. Other difficulties of the irradiation technique occur because of saturation transfer and cross-relaxation. In conclusion, irradiation should be avoided if the field 8_0 is inhomogeneous.

3.1.b Excitation Methods

The selective excitation sequences are numerous. However, some general observations can be made:

- 1. The soft pulse (or long pulse) methods require very fine tuning of B_1 .
- 2. Methods with an even number of pulses (e.g. $1-\overline{3}-3-\overline{1}$) are less sensitive to pulse shape inaccuracies than those with odd numbers (e.g. $1-\overline{2}-1$) because each pulse in one phase is balanced by a pulse of exactly the same length in the opposite phase. (Note: the numbers give relative pulse lengths and the overbar means a 180° shift. The delay time, τ , between pulses is constant.)
- 3. Even sequences are less sensitive to B_0 and B_1 inhomogeneities but are more susceptible to phase shifts.
- 4. Problems with a switching transient may be encountered if the pulse angles are small.
- 5. Sequences involving phase shifts (e.g. 1-1) require very accurate phase shifts and precise balance in the RF channel.
- 6. The longer the pulse sequence, the higher the risk of phase distorsion.

These features enable selection of the most appropriate method for sensing the sugar content of fruits. Generally, soft pulses are more sensitive to B_1 and B_0 inhomogeneities, and cannot be used. Although the DANTE method usually requires very short pulses, it can cause transient errors during switching. For the binomial sequences and methods derived from them, the even sequences are more advantageous than the odd ones because they are less prone to problems of pulse shape. Therefore, they are the preferred methods.

3.2 Relaxation Time Techniques

These techniques attempt to zero the magnetization of the solvent before the acquisition. They are only successful when there is a great difference between the relaxation times of the solute and the solvent. These are the only available methods if the solute and the solvent peak are close because the selectivity is based on the frequency. Unfortunately, these methods often decrease the signal strength and change the relative intensity. As water is a small molecule, its motion may be very fast. Differences are more likely among larger biological molecules (e.g. carbohydrates, fat, etc).

In a water-solute system, if $T_{1(water)} \ll T_{1(solute)}$, a good method of suppressing the water peak is fast pulsing to achieve a steady state. For T_1 methods, a very good B_1 homogeneity is needed so that the solvent magnetization can be zeroed everywhere at the same time. Methods using T_2 differences, such as the Carr-Purcell-Melboom-Gill (CPMG) sequence, are less sensitive to field inhomogeneities, but usually require use of a reactant.

3.3 Choice of Appropriate Technique

Figure 8 is a block diagram illustrating the choice of an appropriate method for water peak suppression. The choice mainly depends on:

- 1. The proximity of the solute and the solvent peaks
- 2. The degree of inhomogeneity of the magnetic fields, B_0 and B_1
- 3. The purpose of the spectrum
 - Is phase error essential?
 - Will the relative intensity be measured?
 - Is saturation transfer important? etc....

References

- [1] Behar K.L., D.L. Rothman, R.G. Shulman, A.O.C. Petorff, J.W. Prichard. 1984. Detection of cerebral lactate in vivo during hypoxemia by H¹ at relatively low field strengths (1.9 T). Proc. Natl. Acad. Sci. USA 81:2571-2519.
- [2] Brown F.F, I.D. Campbell, P.W. Kuchel, D.C. Rabenstein. 1977. *Human erythrocyte metabolism studies by* H¹ *echo NMR*. Federation of European Biochemical Societies (FEBS) 82(1): 12-16.
- [3] Doddrell D.M., G.J. Galloway, W.M. Brooks, J. Field, J.M. Bulsing, M.G. Irving, H. Baddeley. 1986. Water signal elimination in vivo using suppression by mistimed echo and repetitive gradient episodes. J. Magn. Reson. 70:176-180.
- [4] Fukushima E. and S.B.W. Roeder. 1981. Experimental pulse NMR; a nuts and bolds approach. Addison-Wesley Publishing Co. Inc., Reading, MA.
- [5] Hore J.P. 1989. Methods in enymology. Volume 176. Academic Press, New York, NY.
- [6] Hore J.P. 1983. Solvent suppression in Fourier transform nuclear magnetic resonance. J. Magn. Reson. 55: 283-300.
- [7] Jue T., F. Arias-Mendoza, N.C. Gonnella, G.I. Shulman, R.G. Shulman. 1985. A H¹ NMR technique for observing metabolite signals in the spectrum of perfused liver. Proc. Natl. Acad. Sci. USA 82: 5246-5249.
- [8] Levitt M.H., M.F. Roberts. 1987. Solvent signal suppression without phase distortion in High resolution NMR. J. Magn. Reson. 71: 576-581
- [9] Martin M.L., J.J. Delpuech, G.J. Martin. 1980. Practical NMR spectroscopy. Heyden & Son, London, UK.

- [10] Morris G.A. and R. Freeman R. 1978. Selective excitation in Fourier transform Nuclear magnetic Resonance. J. Magn. Reson. 29: 433-462.
- [11] Morris G.A., K.I. Smith, J.C. Watterton. 1986. Pulse sequences for solvent suppression with minimal spectral distorsion. J. Magn. Reson. 68: 526-532.
- [12] Rabenstein D.L. and A.A. Isab. 1979. Water elimination by T₂ relaxation in H¹ spin echo FT NMR studies of intact human erythrocytes and proteins solutions. J. Magn. Reson. 36: 281-286.
- [13] Redfield A.G., S.D. Kunz, E.K. Ralph. 1974. Dynamic range in Fourier Transform Proton Magnetic resonance. J. Magn. Reson. 19:114.
- [14] Starcuk Z., L. Pucek, R. Fiala, Z. Starcuk, Jr. 1988. A new approach to solvent signal suppression giving pure absorption mode spectra. J. Magn. Reson. 80: 344-351.
- [15] Sklenar V., R. Tschudin, A. Bay. 1987. Water suppression using a combination of hard and soft pulses. J. Magn. Reson. 75: 352-357.
- [16] Starcuk Z., V. Sklenar. 1986. New hard pulse for the solvent signal suppression in Fourier Transform NMR.II. J. Magn. Reson. 66: 391-397.
- [17] Starcuk Z., V. Sklenar. 1987. New hard pulse sequence for the solvent signal suppression in Fourier Transform NMR.I. J. Magn. Reson. 61: 567.
- [18] Takahashi S., K. Nagayama. 1989. Method of selective solvent resonance suppression which combines FIDs obtained from 1-1 pulses. J. Magn. Reson. 81: 555-560.
- [19] Ugurbil K., M. Petein, R. Maidan, S. Michurki, J.N. Cohn, A.H. From. 1984. High resolution Proton NMR studies of perfused rat hearts. FEBS 1202, 167(1): 73-78.
- [20] Williams S.R., D.G. Gadian, E. Proctor, D.B. Sprague, D.F. Talbot. 1985. Proton NMR studies of muscles metabolites in vivo. J. Magn. Reson. 63: 406-412.
- [21] Clore G.M., B.J. Kimber, A.M. Growenborg. 1983. The 1-1 Hard Phase: a Simple and Effective Method of Water Resonance Suppression in FT ¹H NMR. J. Magn. Reson. 54:170-173.
- [22] Bellon, V., Cho S.I., Krutz, G.W. 1989. Review on Water Peak Suppression in Pulsed ¹H NMR Spectroscopy. Technical Report. Agricultural Engineering Department, Purdue University, West Lafayette, IN.

Figures

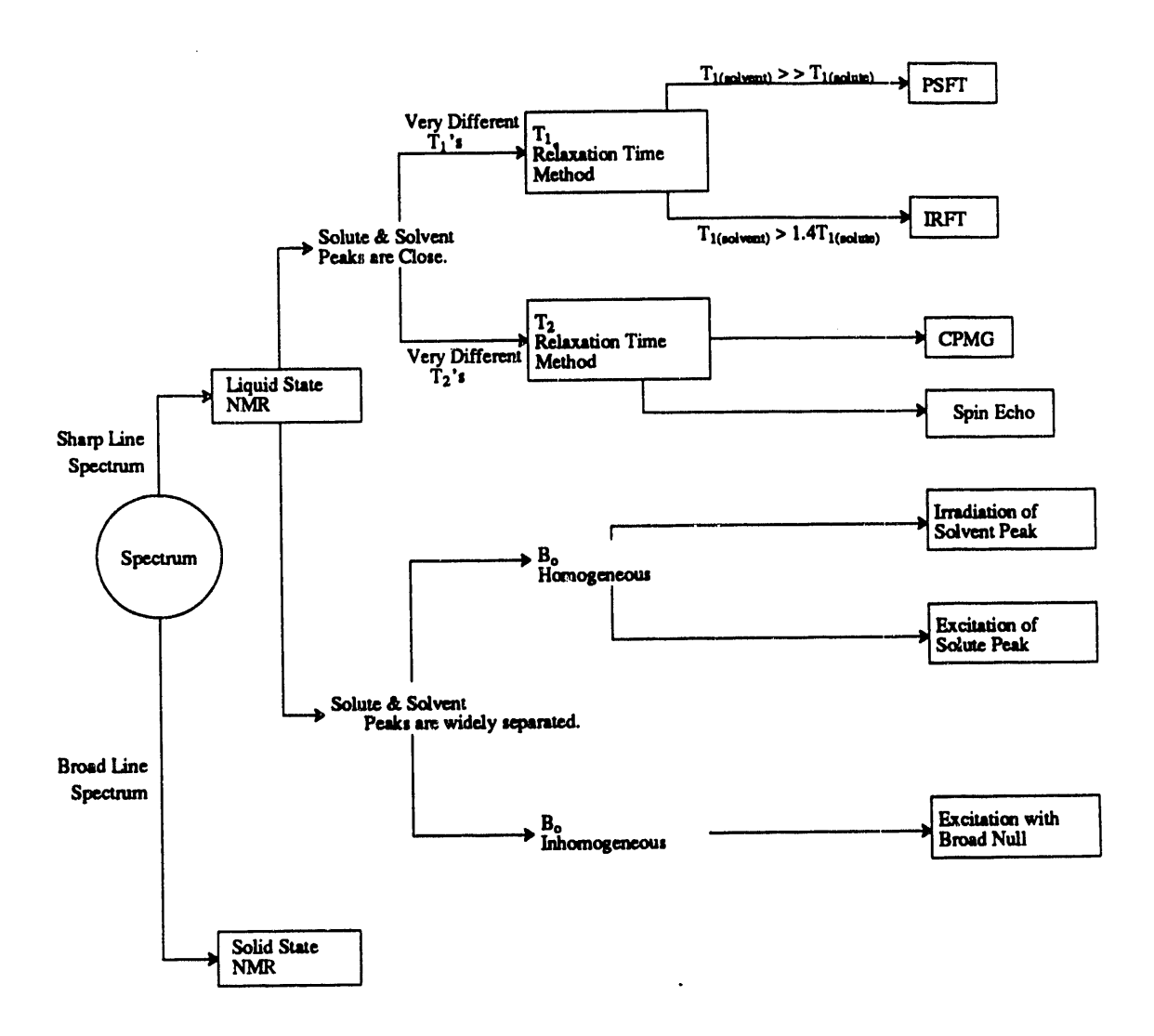


Figure 8. Some criteria for choosing a good water peak suppression method

4. WATER PEAK SUPPRESSION

In the study described in section 2, which employed proton Magnetic Resonance (1 H-MR at 200 MHz), the amplitude of the sugar peak was highly correlated ($r \le 0.99$) with the sugar content of banana and apple tissue (Cho, 1989). Sugar content has been highly correlated with ripeness in most fruit. A design for a low field 1 H-MR ripeness sensor has also been proposed (Cho *et al.*, 1990).

The ¹H-MR spectra of fruit tissue samples include both water and sugar peaks. Because the water content is dominent, the water peak is intense and the sugar peak is relatively weak. The water peak is broad and partially masks the sugar peaks, making quantification difficult. This problem becomes worse when the magnetic field of the spectrometer is low. Therefore, in developing a ripeness sensor based on ¹H-MR with low magnetic fields, the water peak should be suppressed. This section of the report describes an investigation of the feasibility of measuring sugar content in fruit tissue using two relatively simple water peak suppression techniques in a high magnetic field ¹H-MR spectrometer.

The experiments were performed at the Purdue University Biochemical Magnetic Resonance Laboratory, supported by NIH (grant RR01077 from the Biotechnology Resources Program of the Division of Research Resources), and the NSF National Biological Facilities Center on Biomolecular NMR, Structure and Design at Purdue (grants BBS8614177 and 8714258 from the Division of Biological Instrumentation).

4.1 Materials and Methods

A high resolution ¹H-MR spectrometer (Varian Unity 200) which operated at 200 MHz was used to observe the ¹H spectra of muskmelon samples. The room was maintained at 25 °C. The width of a 90° pulse was 24.7 µs and FID (free induction decay) signals were stored as 16K data points. Seven different muskmelons were used; 11 tissue samples from four melons were used for the T₁ (spin-lattice relaxation time) measurements, and 10 samples from three melons were used for the remaining measurements (single pulse, selective saturation, and inversion recovery).

The cored pieces were gently pressed into the glass sample tube to maintain the original tissue structure. The cored fruit tissue was not smashed or otherwise physically changed. The diameter of the sample tube was 5 mm, and was limited by the diameter of the available probe. A refractometer (Atago N_1 , Brix 0-32%) was used to measure sugar content (assumed to be equal to soluble solids content) of all samples. Juice was removed from cored samples by squeezing them between thumb and index finger.

Techniques for water peak suppression were reviewed (Bellon et al., 1989) and two simple techniques, selective saturation and the Inversion Recovery Fourier Transform (IRFT) sequence were tested.

4.2 Spin-lattice Relaxation Times

The objectives of these tests were to determine: (1) whether the T_1 values of water and (2) sugar correlated with sugar content and whether the T_1 values of the sugar and water differed enough to use of

Ripeness Sensor Dev. Water Peak Suppression

the IRFT technique to suppress the water peak. The IRFT technique can only be used when relaxation times vary by at least a factor of 1.4 (Martin et al., 1980).

The measured T_1 relaxation times of water and sugar in muskmelon with different sugar contents varied from 1.86 to 2.7 sec (water) and from 0.53 to 1.3 sec (sugar). The T_1 of water was at least twice as large as the T_1 of sugar in all cases. Therefore, the IRFT pulse sequence could be used for water peak suppression. The samples with higher sugar content had shorter T_1 times. The T_1 values of water and sugar were linearly correlated with sugar content as shown in Figure 9. Correlation coefficients r were 0.76 and 0.82, respectively. Standard errors of calibration (SEC) were 0.202 and 0.160, respectively. The T_1 of sugar was more highly correlated than the T_1 of water.

4.3 Single Pulse

The resonance signal may be detected after a short (μ s) and intense radio frequency pulse B_1 that tilts the total ¹H magnetization by a certain angle relative to the static magnetic field (the z-direction). This creates detectable magnetization in the xy (transverse) plane.

The water resonance strongly dominated the sugar resonance, but these were broadened somewhat due to magnetic inhomogeneity in the tissue. The strong water resonance can cause the apparent signal to noise ratio (S/N) of the sugar resonance to appear to be relatively low. (Note: S/N is the ratio of the height of the water or sugar peak to the height of the noise). Also at low sugar contents it masks the sugar peak. The sugar peak was not visible in unripened muskmelon (sugar content less than 8%). The heights of the sugar peaks were measured and their correlation with sugar content is shown in Figure 10. The r was 0.94 and the SEC was 3.48. The S/N was 15 at 8.3% sugar.

4.4 Selective Saturation with Single Pulse

In the selective saturation experiment, the water resonance was irradiated by an additional radio frequency field B_2 applied as a long (ms) and weak (a few watts) pulse. First a spectrum was recorded and then the B_2 frequency was adjusted to correspond to the peak to be irradiated.

Selective irradiation of the water peak resulted in significant reduction of water resonance intensity, but the shape of the residual peak showed "hole burning". This indicated the original water peak was heterogeneously broadened; that is, it was composed of many overlapping resonances of different frequencies. The existence of inhomogeneous broadening suggested that selective irradiation may not be a suitable technique for suppressing the water peak.

4.5 Inversion Recovery Sequence

The IRFT sequence first rotates the total magnetization of all protons by 180° . Then the 1 H longitudinal (z-component) magnetization is allowed to partially relax (i.e. to approach initial equilibrium) during a delay time τ_{2} . After the delay a 90° pulse is applied to create detectable transverse magnetization. The resonance signal is detected immediately following the 90° pulse. The difference in the spin-lattice relaxation times, commonly referred to as T_{1} , can be used to suppress the water peak. Water protons relax more slowly than sugar protons (i.e. longitudinal relaxation time T_{1} is greater for water protons), and at a time τ_{2} the water signal is zero whereas the sugar signal has recovered to positive values. When the signal is measured at that time, the water peak is suppressed.

The delay time τ_2 is dependent on the particular longitudinal relaxation times T_1 of both water and sugar. The longitudinal relaxation times of both were measured in a separate experiment to confirm that $T_{1(water)} > 1.4 \ T_{1(sugar)}$ and to determine the optimal value of τ_2 . The most appropriate τ_2 time for effective water peak suppression apparently was between 1 and 1.2 sec. The delay time chosen was 1.2 sec, which generally resulted in no "wings" on the water peak.

Peaks were detectable with the IRFT technique for samples with sugar contents as low as 1.8%. The spectral criterion was the absolute height of the sugar peak. As shown in Figure 11, two regression models were tested: a linear regression, which gave an r of 0.94 and standard error of correlation (SEC) of 19.64, and a polynomial regression, which gave an r of 0.98 and an SEC of 12.70. The correlation coefficient r for the linear regression was as high as those obtained with the single pulse method. Furthermore, in this experiment measurements were obtained from all 10 samples over a wider sugar concentration range. The S/N ratio was about 34 at 8.3% sugar content, considerably higher than in the single pulse experiment.

4.6 Summary of Significant Findings

The sugar content of fruit tissue cores was measured using the sugar proton resonance intensity in the high resolution (pulsed FT) 1 H-MR spectra. The $T_{1(water)}$ was almost twice that of $T_{1(sugar)}$, allowing a T_1 -selective (IRFT) pulse sequence to be applied to suppress the strong water resonance. With the single pulse method, sugar peaks in fruit tissue with low sugar content (less than 8%) were not detectable. However, the IRFT pulse sequence effectively suppressed the strong water resonance (relative to sugar resonance intensity) in all fruit samples and significantly improved the S/N ratio of the sugar peak, allowing detection of the sugar peak in a fruit sample having a sugar content as low as 1.8%. Calibration plots between refractometer measurements of sugar content and sugar peak height were obtained using both the single pulse and the IRFT pulse sequence. The data acquisition time to obtain an 1 H-MR spectrum was less than 1 second with the single pulse technique and less than 2 seconds with the IRFT pulse.

References

- [1] Bellon, V., and Boisde, G. 1989. Remote Near Infrared Spectroscopy in Food Industry with the use of silica and fluoride glasses fibers. pg. 350-359 in: Proceedings of the conference SPIE. January 17-19, 1989, Los Angeles, CA.
- [2] Bellon, V., Cho S.I., Krutz, G.W. 1989. Review on Water Peak Suppression in Pulsed ¹H NMR Spectroscopy. Technical report. Agricultural Engineering Department, Purdue University, West Lafayette, IN.
- [3] Belton, P.S., Colquhoun, I.J. 1989. Nuclear Magnetic Resonance Spectroscopy in Food Research. Spectroscopy 4(2): 22-32
- [4] Cho, S.I. 1989. Development of a Nuclear Magnetic Resonance Based Sensor Development to Detect Ripeness of Fruit. Unpublished Ph.D. dissertation, Agricultural Engineering, Purdue University, West Lafayette, IN.
- [5] Cho, S.I., Krutz, G.W., Gibson, H.G., and Haghighi, K. 1990. Magnet Console Design of an NMR Based Sensor to Detect Ripeness of Fruit. ASAE Transactions, 33(4):1043-1050.

- [6] Dull, G.G. 1986. Nondestructive evaluation of quality of stored fruits and vegetables. Food Technol. 40(5):106-110.
- [7] Dull, G.G., Birth, G.S., Smittle, D.A., Leffler, R.G. 1989. Near Infrared Analysis of Soluble Solids in Intact Cantaloupe. J. Food Sci. 54(2):393-395.
- [8] Edzes, H., Samulski, E.T. 1978. The Measurement of Cross-Relaxation Effects in the Proton NMR Spin-Lattice Relaxation of Water in Biological Systems; Hydrated Collagen and Muscle. J. Magn. Reson. 31(2): 207-229.
- [9] Gadian, D.G. 1982. Nuclear Magnetic Resonance and its Application to Living Systems. Clarendon Press, Oxford, UK.
- [10] Martin, M.L., Delpuech, J.J. and Martin, G.J. 1980. Practical NMR Spectroscopy. Heydon and Sons, Ltd., London, UK.
- [11] Rutar, V., Kovac, M., Lahajnar, G. 1988. Improved NMR Spectra of Liquid Components in Heterogeneous Samples. J. Magn. Reson. 80(1):133-138.
- [12] Zind, T. 1990. Fresh Trends '90, A profile of Fresh Produce Consumers. The Packer 97:37-66.



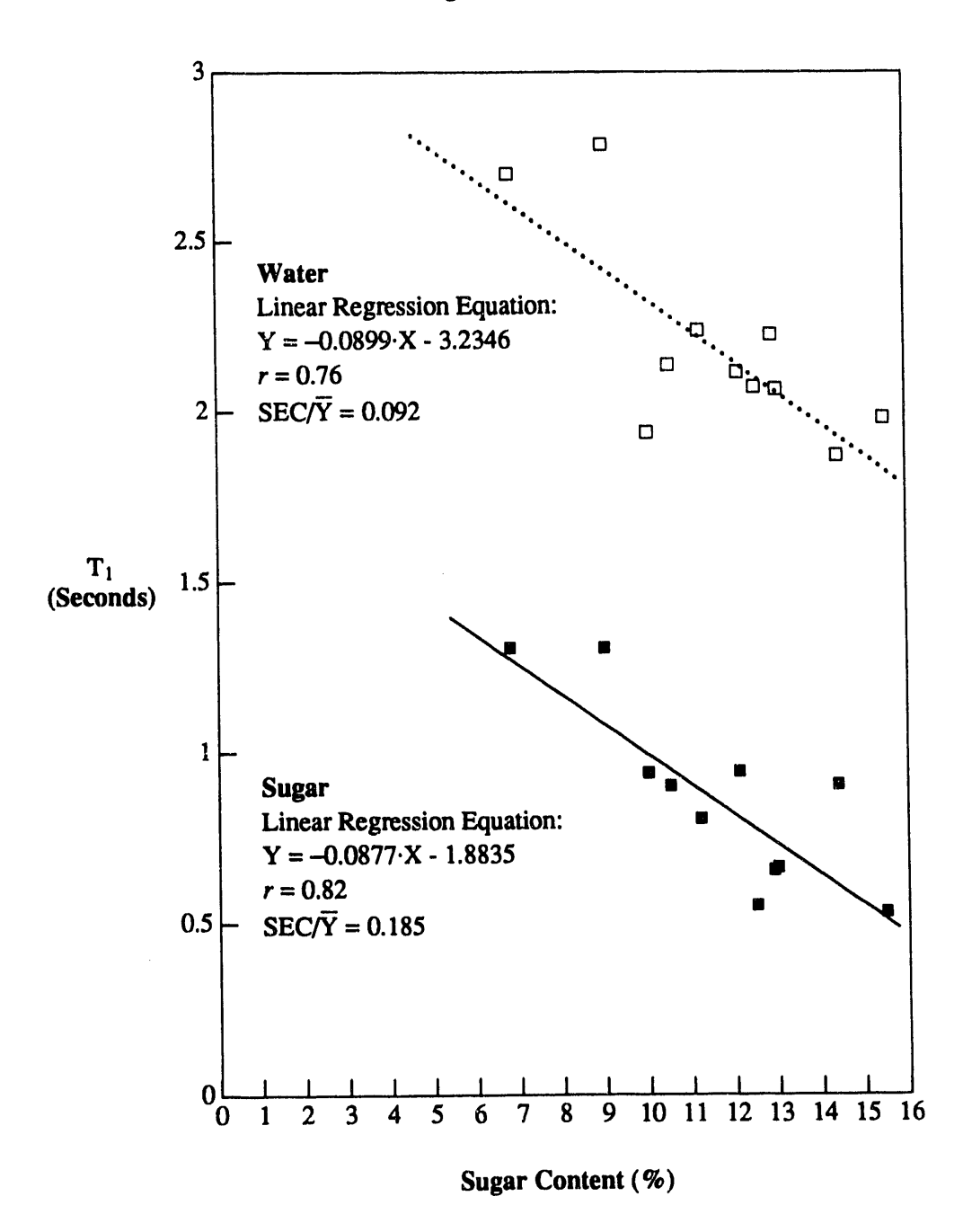


Figure 9. Correlation between hydrogen T_1 (of water and sugar resonances) and refractometer measurements of sugar content in muskmelon.

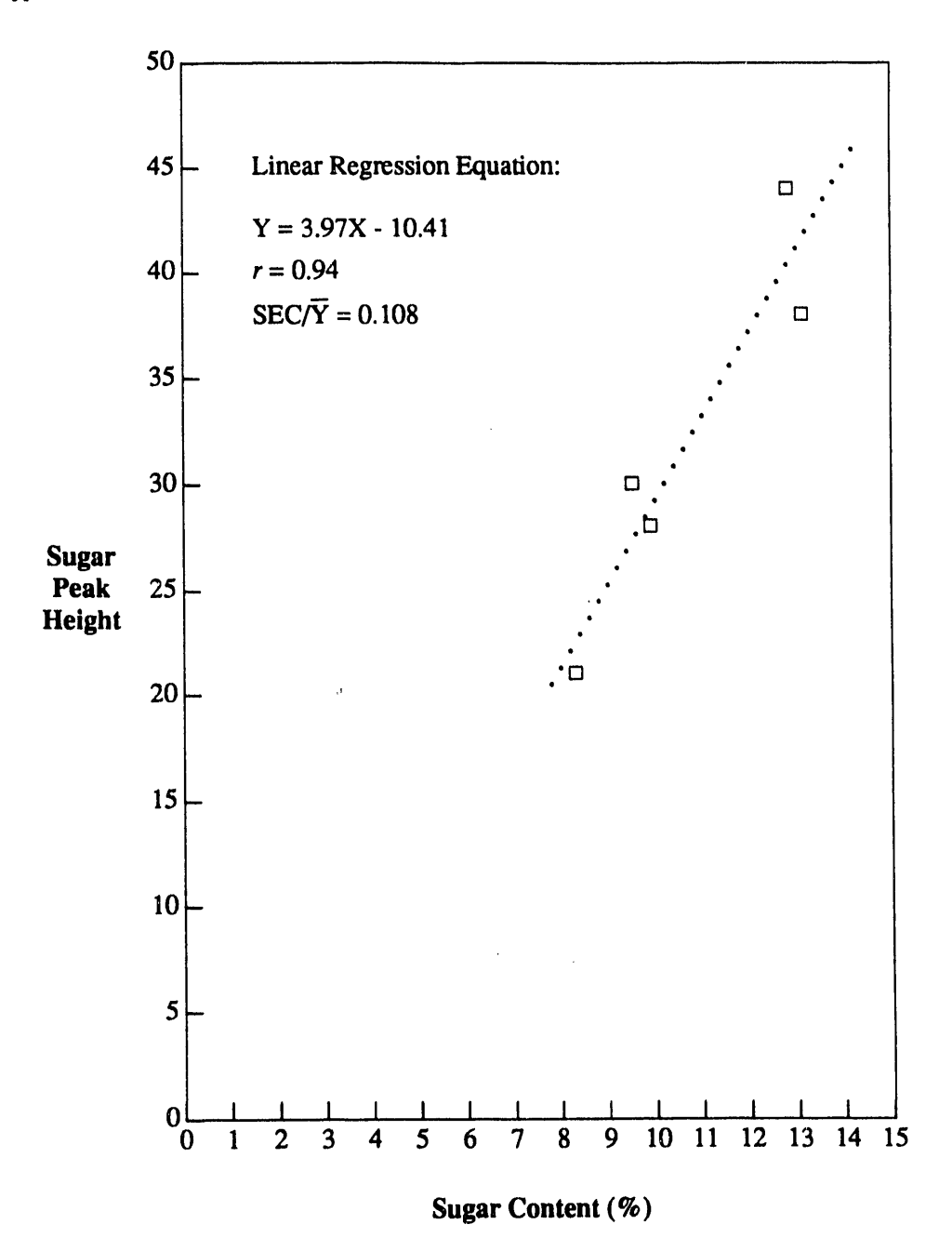


Figure 10. Correlation between ¹H-MR sugar peak height and sugar content in muskmelon using the single pulse technique.

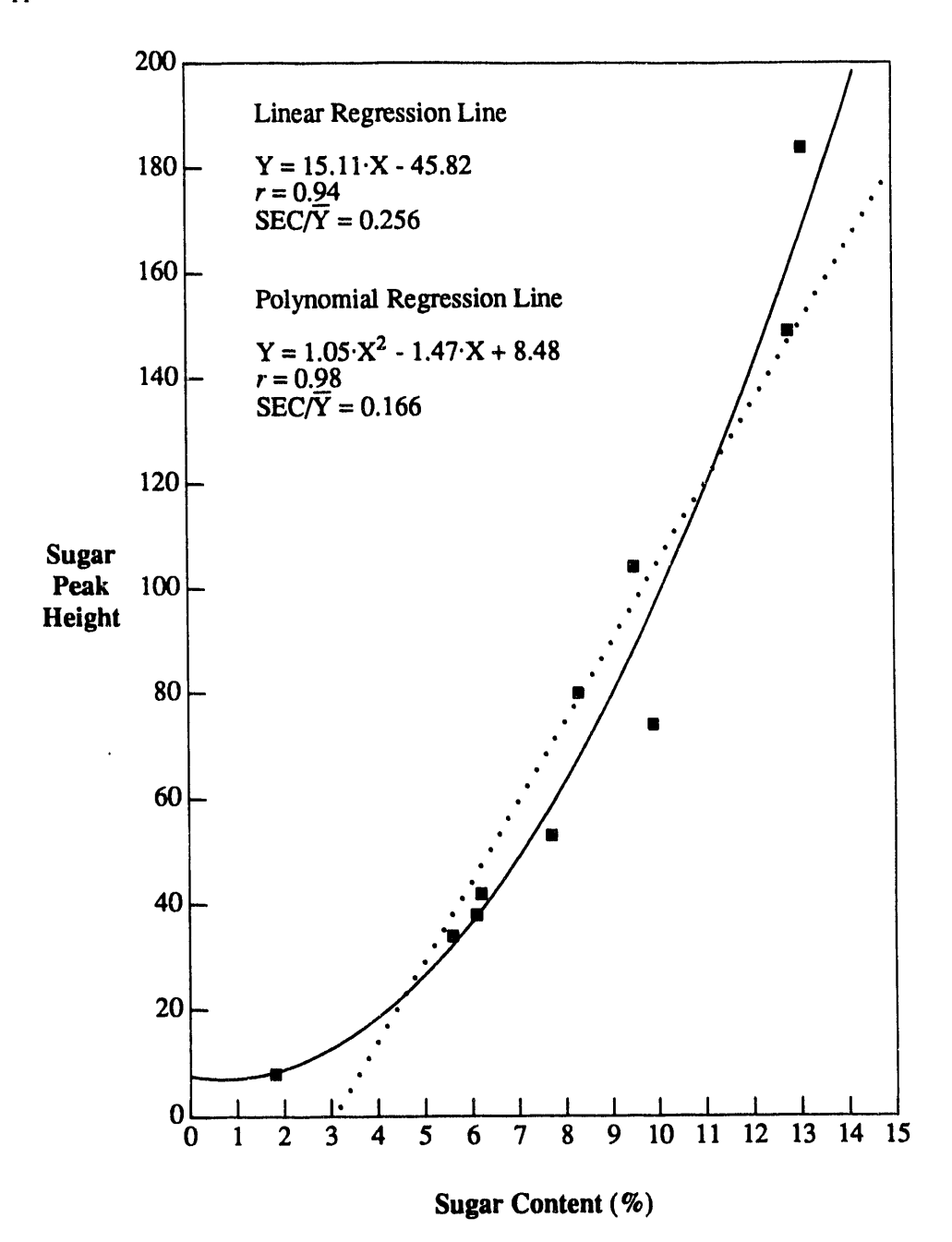


Figure 11. Correlation between ¹H-MR sugar peak height and sugar content in muskmelon tissue using the IRFT pulse technique.

5. NON-DESTRUCTIVE TESTS ON INTACT FRUIT

The experiments described in this section measured the sugar content of intact fruit with low resolution (i.e. low magnetic field) 1 H-MR using the spin-spin (T_2) relaxation time (Martin *et al.*, 1980) of the resonance signal. The specific objectives were (1) to develop a correlation model between T_2 and sugar content using chemical exchange as a basis and (2) to validate the model with 1 H-MR experiments on intact fruit (grapes and cherries).

5.1 Chemical Exchange and Correlation Model

In fruit, sugar is dissolved in water which is in the vacuoles of cells (Lee, 1983). The sugar molecules (such as sucrose, D-glucose, and D-fructose) contain -OH groups having protons that exchange with the protons in water. A sucrose molecule consists of two monosaccharide units (D-glucose and D-fructose) and has a molecular weight of 342 compared to a molecular weight of 18 for H₂O. During the formation of sucrose crystals, three of the eight hydroxyl protons are involved in the formation of intra-molecular bonds and the remaining five are involved in inter-molecular hydrogen bonds. However, during solubilization in water, some of the inter- and intra-molecular bonds are broken (Mora and Baianu, 1990). When considering the concentration of exchangeable protons, water has two moles of exchangeable protons per mole while sucrose has eight moles per mole.

A glucose and a fructose molecule has a molecular weight of 180. A sucrose molecule consists of two monosaccharide units (D-glucose and D-fructose) and has a molecular weight of 342 compared to a molecular weight of 18 for H_2O . In the following, "W" represents water and "S" sugar. A typical yellow banana has 75.7% water and 19.6% sugar (8.5% sucrose, 5.9% fructose and 5.2% glucose) (Ensminger et al., 1983). The number of moles of water, sucrose, fructose and glucose are 4.21, 2.49· 10^{-2} , 3.28· 10^{-2} and 2.89· 10^{-2} , respectively. The proportion of exchangeable protons in water and sugar, i.e. P_W and P_S are 0.943 and 0.057.

The equation that describes $1/\Gamma_{2(obs)}$ when $P_S \ll P_W \approx 1.0$ was given by Martin et al. (1980) in a study of the absorption signal:

$$\frac{1}{T_{2(\text{obs})}} \approx \frac{1}{T_{2W}} + \frac{P_S}{\tau_S} \cdot \frac{T_{2S}^{-2} + (T_{2S} \cdot \tau_S)^{-1} + (\omega_W - \omega_S)^2}{(T_{2S}^{-1} + \tau_S^{-1})^2 + (\omega_W - \omega_S)^2}$$
[1]

where, T_{2W} and T_{2S} are T_2 relaxation times of W (water) and S (sugar), P_W and P_S are proportions of W (water) and S (sugar), ω_W and ω_S are resonance frequencies of W and S, and τ_S is the lifetime on site S (sugar) defined as the time for instantaneous magnetization transfer from S to W.

Chemical exchange is considered to be very fast if $\tau_S^{-1} \gg$ both T_{2S}^{-1} and $(\omega_W - \omega_S)$. In 1H -MR spectrum, the water and sugar peak are separated by about 1 ppm. For 10 MHz 1H -MR, $\omega_W - \omega_S = 10$ MHz· $10^{-6} = 10$ Hz. Also $T_{2S}^{-1} \approx 1$ Hz, because $T_{2S} \approx 1$ sec for a dilute sugar solution (Mora and Baianu, 1989, 1990). Generally, the exchange between the hydroxyl protons of water and sugar is very fast and the residence time at each site is always smaller than 1 ms. Therefore, the exchange rate τ_S^{-1} will be greater than 1000 Hz and $\tau_S^{-1} >>$ both T_{2S}^{-1} and $(\omega_W - \omega_S)$. In the case of very fast exchange, equation [1] becomes

$$\frac{1}{T_{2(\text{obs})}} \approx \frac{1}{T_{2W}} + P_{S} \cdot \left[\frac{1}{T_{2S}} + \tau_{S} \cdot (\omega_{W} - \omega_{S})^{2} \right].$$
 [2]

The third term, $P_S \cdot \tau_S \cdot (\omega_W - \omega_S)^2 \ll 1.0$, and can be negligible. Equation [2] can be expanded in the binomial series $(1+x)^{-1}$ and higher order terms can be ignored. For sugar contents typically found in fruits, banana has highest sugar content. Therefore, P_S of banana has a maximum value, or 0.057. We know that $T_{2S} \approx 1$ sec for a dilute sugar solution (Mora and Baianu, 1989, 1990). T_{2W}/T_{2S} is usually less than 2.0. Therefore, equation [2] becomes

$$T_{2(obs)} \approx T_{2W} \cdot [1 - \frac{T_{2W}}{T_{2S}} \cdot P_S + (\frac{T_{2W}}{T_{2S}} \cdot P_S)^2].$$
 [3]

The P_S² term is nearly negligible, because P_S << 1. Free sugar in sweet cherries and grapes consists of fructose snd glucose. For example, ripe grapes have 81.6% water, 0.2% sucrose, 4.3% fructose and 4.8% glucose and ripe sweet cherries have 80.4% water, 1.9% sucrose, 7.2% fructose and 4.7% glucose (Ensminger et al., 1983). The amount of sucrose is negligible. In this case, the value of Ps is calculated as follows:

$$P_{S} = \frac{5 \cdot C/180}{5 \cdot C/180 + 2 \cdot (100 - C)/18}$$
 [4]

where, C is the sugar content in percent weight. Because the sugar content of fruit is less than 25%, $5 \cdot \text{C}/180 \ll 2 \cdot (100 - \text{C})/18$. Therefore, $5 \cdot \text{C}/180$ can be eliminated from the denominator. Using the binomial series approximation and substituting P_S gives an expression for T_{2(obs)} as a function of the three parameters X, Y and measured sugar content C (%) of intact fruit:

$$T_{2(obs)} \approx X - \frac{Y}{400} \cdot C - \frac{Y}{40000} \cdot C^2$$
 [5]

Because the sugar content in fruit is less than 25%, the third term containing C² in equation [5] becomes negligible, and the expression becomes approximately linear: $T_{2(obs)} \approx X - \frac{Y}{400} \cdot C = X - \frac{Y}{4} \cdot \frac{C}{100}$

$$T_{2(obs)} \approx X - \frac{\hat{Y}}{400} \cdot C = X - \frac{Y}{4} \cdot \frac{C}{100}$$
 [6]

where, $X=T_{2W}$ and $Y=T_{2W}^2/T_{2S}$. Therefore, equation [6] is a correlation model which suggests that measured T_2 is linearly correlated to sugar content C (%). The intercept X implies the value of T_{2W} .

5.2 Experimental Evidence for the Correlation

Intact berries of "Red Flame Seedless" grapes and sweet cherries (grown in Washington and California) were tested with a Bruker 10 MHz Pulsed ¹H-MR spectrometer (Model PC-10). The inside diameter of the sample tube was 24 mm. The intermediate diameter of the grapes and cherries ranged from 22 to 24 mm. The average weights of the grapes and the cherries were, respectively, 4.712±0.487 g and 5.652±0.459 g. A refractometer (Atago N₁, Brix 0-32%) was used to estimate sugar content of the samples. Juice for the refractometer measurement was obtained by squeezing the samples by hand.

T₂ is called the spin-spin relaxation time and is the time constant of the FID resonance signal. T₂ values were measured with the Carr-Purcell-Meiboom-Gill (CPMG) pulse sequence (Martin et al., 1980). Measurements were carried out at 23 ± 1 °C. The time required for T_2 measurement was about 3 sec per scan including the time for 100 echoes of 20 ms and for data acquisition. For each cherry and grape, the T₂ time was measured twice and average values were used.

The correlation between sugar content and measured T_2 was investigated as a means of varidating the correlation model. Figures 12 and 13 show the correlations between observed T_2 values and sugar contents for tests conducted on 17 grapes and 40 cherries. The measured T_2 was linearly correlated to sugar content as suggested by the correlation model (equation [10]). The correlation coefficients r were 0.66 and 0.62 respectively. The standard errors of correlation (SEC) were 0.0197 and 0.0502, respectively.

Firmness is a major quality attribute of many fruits and vegetables. In the tests on sweet cherries, firmness (apparent modulus of elasticity) was also measured using the compression testing procedure described in ASAE Standard S368.2 (ASAE, 1990). Firmness was correlated with T_2 (r=0.6 to 0.7) (Stroshine at al., 1990). Therefore, both sugar and firmness affect T_2 . Additional experiments are needed to determine the 1H -MR device setting and techniques which will give the highest correlations for each of these two factors. It seems possible that firmness and sugar content can be measured simultaneously on an 1H -MR device.

5.3 Conclusions

A correlation model, based on the principle of chemical exchange, predicted that there would be a linear relationship between T_2 and sugar content in intact fruit. This type of relationship was found in ${}^1\text{H-MR}$ tests on intact grapes and cherries. It seems likely that the correlation could be improved by appropriate choice of pulse techniques, separate measurements of both short T_2 and long T_2 , and a probe designed for intact fruit. The results suggest that sugar content in intact fruit can be non-destructively estimated using the T_2 value as determined with low resolution ${}^1\text{H-MR}$ and a ripeness sensor based on low resolution ${}^1\text{H-MR}$ (having a low magnetic field) is feasible.

References

- [1] ASAE. 1990. Compression test of food materials of convex shape. Standard S368.2. ASAE Standards, 37th Edition. American Society of Agricultural Engineers, St. Joseph, MI.
- [2] Cho, S.I. and G.W. Krutz. 1989. Fruit ripeness detection by using ¹H NMR. ASAE paper 89-6620. American Society of Agricultural Engineers, St. Joseph, MI 49085-9659.
- [3] Gadian, D.G. 1982. Nuclear magnetic resonance and its application to living systems. Oxford Univ. Press, New York.
- [4] Lee, F.A. 1983. Basic food chemistry. 2nd ed. The AVI Publishing Company, Inc. Westport, Conn.
- [5] Janick, Jules. 1988. Horticulture, science, and society. HortScience, 23:11.
- [6] Martin, M.L., J.J. Delpoech and G.J. Martin. 1980. Practical NMR spectroscopy. Heyden & Son Ltd, London.
- [7] Mora A. and I.C. Baianu. 1990. Hydration studies of maltodextrins by proton, deuterium and oxygen-17 nuclear magnetic resonance. J. Food Sci. 55(2):462.
- [8] Mora, A. and I.C. Baianu. 1989. ¹H NMR relaxation & viscosity measurements in solutions and suspensions of carbohydrates and starch from corn: the investigation of carbohydrate hydration, sterochemical and aggregation effects in relation to ¹⁷O and ¹³C data for carbohydrate solutions. J. Agric. Food Chem. 38:1459.

Ripeness Sensor Dev.
Non-destructive Intact

[9] Stroshine, R.L., S.I. Cho, and C.L. Griesser. 1989. Measurement of cherry firmness using proton magnetic resonance (oral report). Cherry Firmness Conference held October 30, 1990 in Prosses, Washington. Sponsored by the Washington Tree Fruit Research Commission, White Salman, Washington.

il



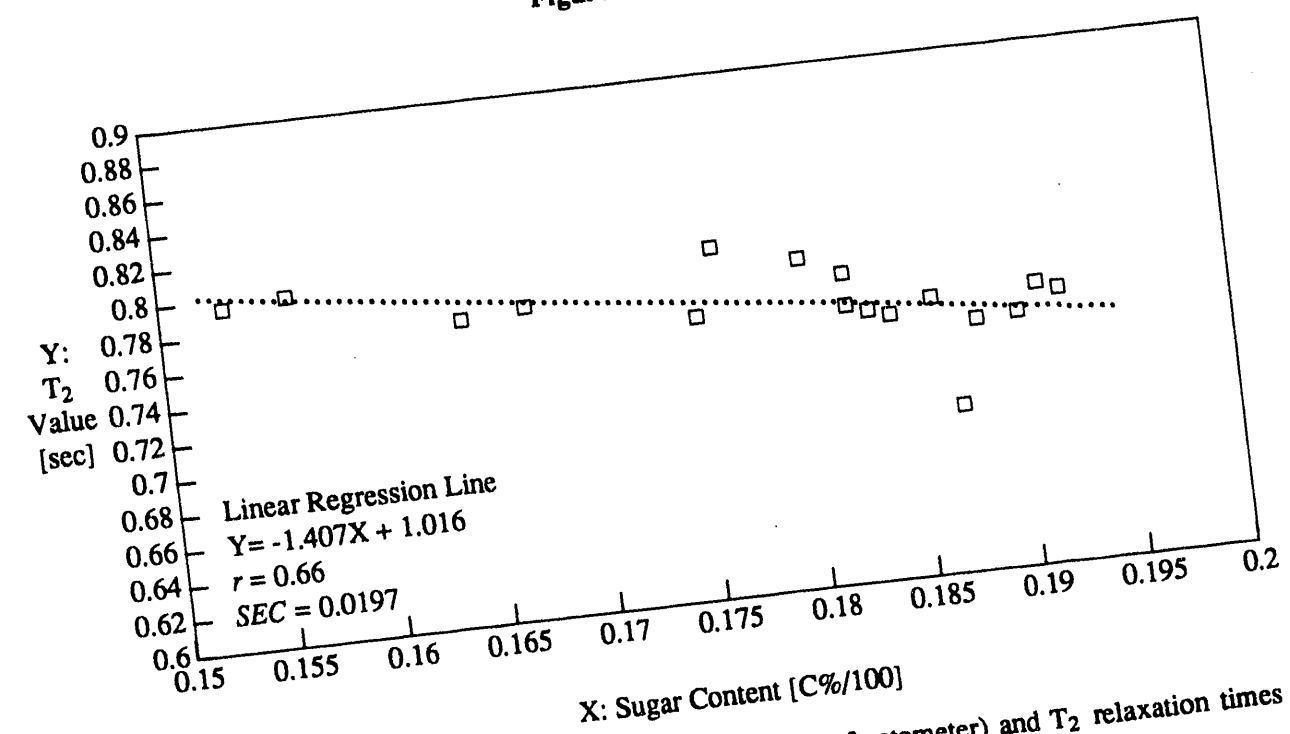
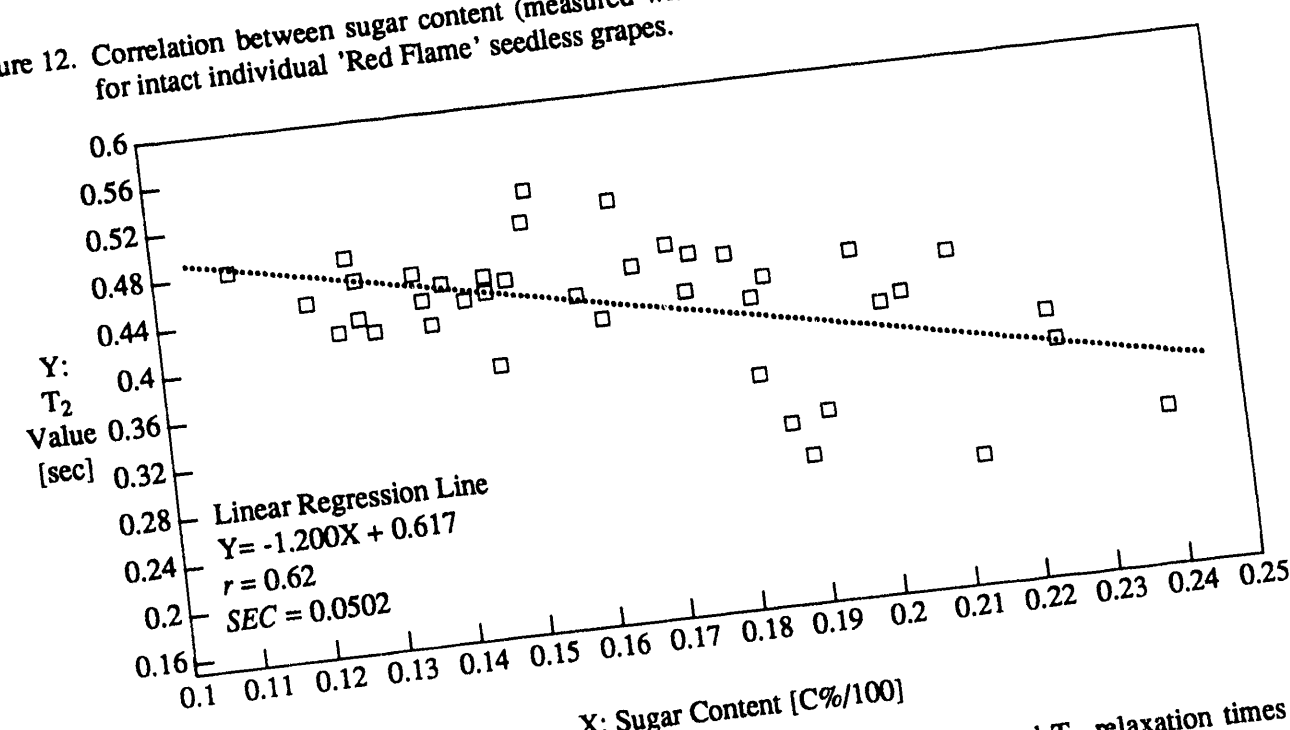


Figure 12. Correlation between sugar content (measured with a refractometer) and T₂ relaxation times



X: Sugar Content [C%/100]

Figure 13. Correlation between sugar content (measured with a refractometer) and T₂ relaxation times for intact Washington sweet cherries.

6. RIPENESS SENSOR DEVELOPMENT: PROTOTYPE

Sections 2, 4 and 5 have described the non-destructive measurement of sugar content in both fruit tissue (core samples) and intact fruit using ¹H-MR. These tests demonstrated the feasibility of developing a ¹H-MR based sensor for non-destructive quality control of fruit. Using a low magnetic field (or permanent magnet) and water peak suppression techniques (for the *second generation* sensors), a low cost (¹H-MR based) sensor is being developed. The prototype ripeness sensor consists of following five main units which are connected as shown in Figure 14:

- 1. Magnet permanent magnet assembly, and steel cover.
- 2. Probe RF (radiofrequency) coil and detect coil, sample tube, and tuning circuit.
- 3. Transmitter signal and pulse generator, pulse programmer, RF gate, and RF power amplifier.
- 4. Receiver RF preamplifier & amplifier, phase-sensitive RF detector, filter, and A/D converter.
- 5. Computer data acquisition, signal processing software, and plotter.

6.1 Magnetic Console Design

The magnetic console box consists of two permanent magnet assemblies and a steel cover. Figure 15 shows the proposed design. Pole surface plates and shimming frames were used to improve the homogeneity. An interactive graphics simulation of a finite element model (FEM) was used to determine an optimal design for the magnet console. This design gave the desired magnetic field strength and homogeneity. Using the FEM simulation, the dimensions and shape of the magnetic console could easily be modified.

A gauss meter providing DC and AC field readings from ± 0.1 gauss to ± 19.99 Kgauss was used to measure the magnetic fields. It gave actuated RMS readings up to 20 KHz. A transverse probe with a 1×2 mm active area was attached to the gauss meter. The resolution of the gauss meter was 0.5 gauss when measuring in the range of 1,000 gauss. Therefore, it did not provide accurate measurements of homogeneity.

A small magnet console was built first. The magnetic fields were measured and compared to the FEM predictions. A ceramic 5 (b_r =3,950 gauss and H_c =192 KAm⁻¹, at 20°C) permanent magnet was used. The air gap was 2 in and small fruit (such as grapes, blueberries, etc.) could be inserted into the air gap which accommodated a 1 in diameter sample tube. The magnet was 4 in wide, 6 in long and 1 in thick. The measured magnetic field intensity was about 1,014 gauss at the air-gap center and the predicted value was 966 gauss. Agreement between the experiment and the FEM simulation was good with a maximum error of 4.7%. This validated the simulation and demonstrated that the FEM program could be used for the magnetic fields were measured at each point (for a 0.25 in matrix). The maximum deviation within this radius was about 2.0 gauss. The predicted maximum deviation was about 1.3 gauss.

Ripeness Sensor Dev. Ripeness Sensor

For the larger magnet console, Ferrimag ceramic 8 permanent magnets (b_r =3,900 gauss and H_c =240 KAm⁻¹, at 20°C) were assembled by using a special glue. The console is 12 in long, 12 in wide and 3 in high. A low carbon steel plate (2 in thickness) was used for the cover. The air gap is 4 in and medium size fruits can be tested using a 2 in sample tube. The measured magnetic field strength was about 1,258 gauss at the air-gap center. The FEM simulation predicted 1,222 gauss which is an error of 2.9%. The measured homogeneity was approximately 300 ppm or less (the sensitivity of the gauss meter was 0.5 gauss) within a 2 in radius of the center of the air-gap. The predicted homogeneity was about 180 ppm.

6.2 Probe Design

The probe represents an interface between magnet, transmitter, and receiver. It is usually a cylindrical form inserted into the air gap of the magnet console and made of a non-magnetic material such as glass or aluminum. The probe also contains a coil of copper wire and a tuning circuit that is required for efficient signal detection. The SPICE circuit simulation program was used to predict the combined impedance of the probe and tuning circuit.

The key component of the probe is the coil of wire that either surrounds the sample or is located adjacent to the sample. Acting as an RF (radio frequency) coil, it transmits radiofrequency power into the sample in the form of an RF induced magnetic field B₁. It also acts as a detect coil which detects the resonance signals from the sample. Therefore, one coil serves as both an RF coil and a detect coil.

Two solenoidal coils were built using copper wire: a 2.0 in diameter and a 1.0 in diameter coil. Copper wire (#16 gage) was selected for the RF/detect coil, because copper has high conductivity and can be readily obtained at high purity. The copper wires were wound around a glass sample tube. The inside diameter was 1.0 in for the small magnet console and 2.0 in for the large magnet console. The thickness was 0.16 in. The probe was positioned in the center of the air-gap between the two magnets.

A serial tuning circuit (Figure 16) was built for efficient power transfer between the detect coil and the pre-amplifier of the receiver unit. The tuning capacitance (C), the inductance (L) of the RF/detect coil, and the resonance frequency ω_0 have the following relationship:

$$\omega_0^2 = 1/LC_1 \tag{7}$$

At resonance, the induced electrical signal is amplified by the quality factor Q of the tuning circuit. The RF energy induced in the tuned coil by the sample is then transferred to a preamplifier. For the small magnet console, the resonance frequency (m_0) is 4.25 MHz, the inductance (L) of the coil is 6.5 μ H, and the resistance (R) is 0.2 Ω . Therefore, the quality factor Q of the tuning circuit is:

$$Q = \frac{L\omega_o}{R} = 890$$
 [8]

6.3 RF Transmitter Circuits

The RF pulse sequences were generated by the programmable function/signal generator and controlled by the PC. The signal generator is capable of producing both pulse and continuous waves and mixing them simultaneously. The control line which triggers the signal generator is connected to the TRIGIN input from the PC which initiates the desired RF pulses. The amplitude and width of the RF pulse as well as the frequency of the RF signal are controlled by programming the function/signal generator from the front panel.

Ripeness Sensor Dev. Ripeness Sensor

To create a sufficient amount of alternating magnetic field inside the probe a current of 1 to 5 amperes is needed. The specific amount of power needed depends on the impedance of the probe tuning circuit. An RF power amplifier must be connected to the output of the signal generator. It is capable of supplying 50 to 150 watts of power. A series of back-to-back diodes (Figure 16) was used to get sharp RF pulses (pulses which looked as nearly as possible like square waves).

6.4 Receiver Circuits

The receiver circuit (Figure 16) consists of a pre-amplifier, an amplifier and interface circuits. Resonance signals in the range of several microvolts ($\mu\nu$) are received from the tuning circuit. This signal is a Frequency Modulation of the two signals. The carrier frequency will be the same frequency as the RF signal used to excite the sample and the resonance signal ranges from 1 to 5 KHz. Thus, the amplifiers used must be operable for frequencies of up to 5 MHz. The envelopes of the resonance signals are transmitted from the interface circuit to a digitizer for data acquisition. However, the resonance signals can be examined by connecting an oscilloscope (having a storage function) to the "A" point in Figure 16.

6.5 Computer and Data Acquisition Board

A 25 MHz/386 IBM PC is used to process output signals via a DAS16G1 data acquisition and control board. A program for the PC was written to (a) trigger the pulse generator, (b) digitize the signals in 16 bits at a high speed (20,000 to 70,000 samples per second), and (c) plot the signals. The gain for the high resolution A/D converter, the delay time, the sampling rate, the sampling time, and the accumulation rate were also controlled by the program.

References

- [1] Cho, S.I., G.W. Krutz, H.G. Gibson and K. Haghighi. 1990. Magnet Console Design of an NMR-based Sensor to detect ripeness of fruit. ASAE Transactions 33(4):1043-1050.
- [2] Clark, W.G. 1964. Pulsed nuclear resonance apparatus. Rev. Sci. Instrum. 35(3):316-333.
- [3] Clark, W.G. and J.A. McNeil. 1973. Single coil series resonant circuit for pulsed nuclear resonance. Rev. Sci. Instrum. 44(7):844-851.
- [4] Farrar, T.C. and E. Becker. 1971. Pulsed and Fourier Transform NMR: Introduction to Theory and Methods. Academic Press, N.Y.
- [5] Halbach, R.E., J.H. Battocletti, and A. Sances, Jr. 1979. Cylindrical crossed-coil NMR limb blood flowmeter. Rev. Sci. Instrum. 50(4):428-434.
- [6] Hoult, D.I., and R.E. Richards. 1976. The signal-to-noise ratio of nuclear magnetic resonance experiment. J. Magn. Reson. 24:71-85.
- [7] Jones, D.E. 1970. Part 1: Nuclear Magnetic Resonance Studies of Metal Ion-Nucleotide binding. Part II: Carbon-13 Pulse Nuclear Magnetic Resonance. Ph.D. Dissertation. University of California, Berkeley.
- [8] Gadian, D.G. 1982. Nuclear magnetic resonance and its applications to living systems. Clarendon Press, Oxford, UK.

Ripeness Sensor Dev. Ripeness Sensor

- [9] Kan, S., P. Gonord, C. Duret, J. Salset, and C. Vibet. 1973. A versatile and inexpensive electronic system for a high resolution NMR spectrometer. Rev. Sci. Instrum. 44(12):1725-1733.
- [10] Martin, M.L., J.-J. Delpuech, and G.J. Martin. 1980. Practical NMR spectroscopy. Heyden & Son Ltd, London, UK.
- [11] Sindorf, D.W. and V.J. Bartuska. 1989. Wide-line NMR spectroscopy in solids using variable frequency pulses. J. Magn. Reson. 85;581-585.

Figures

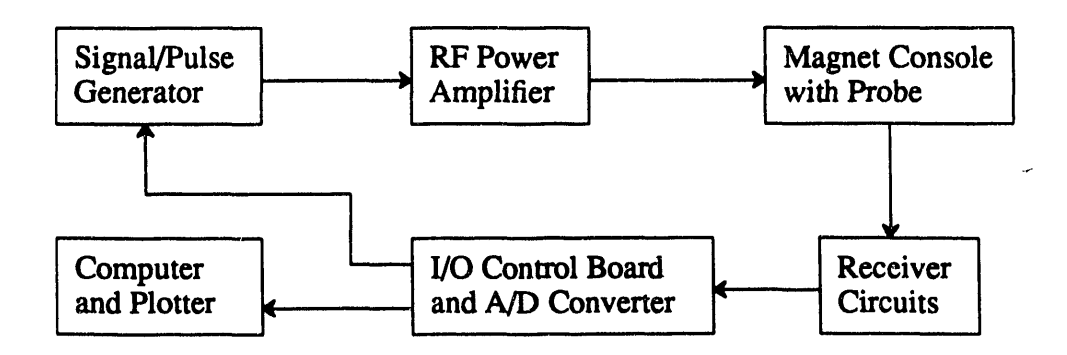


Figure 14. Schematic diagram of the prototype ripeness sensor

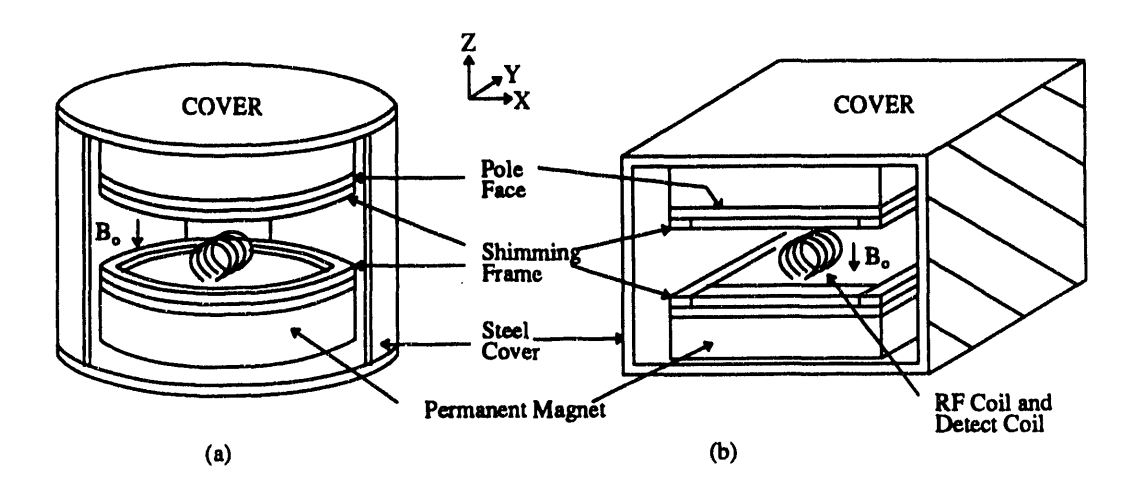
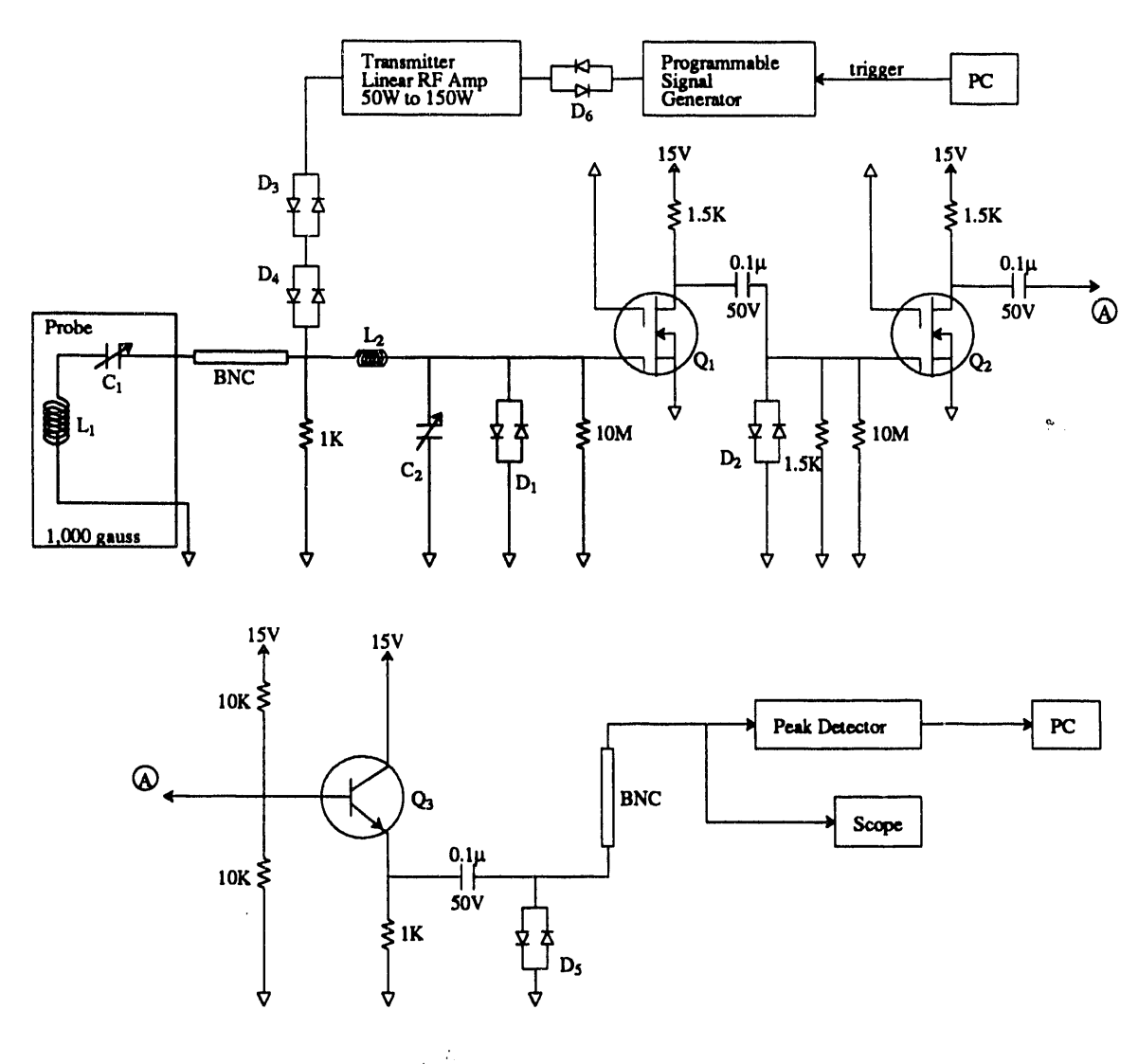


Figure 15. The magnet console configuration of the ¹H-MR based sensor



 L_1 = Sample Coil, 6.5 μ H

 $L_2 = \text{Coil}$ (not air coil), 6.5 μH

 C_1 , C_2 = Tuning capacitors, 95 pF to 42 pF, 110 V_{max}

 D_1 , D_3 , D_4 , D_5 , D_6 = Back-to-back diode, IN4448

D₂ = Back-to-back diode, NTE519 (equivalent to IN3600)

 $Q_1, Q_2 = MFE211$

 $Q_3 = 2N2222$

Gain of cascading Q_1 , Q_2 & Q_3 is about 50 to 100.

Figure 16. Circuit diagram for the prototype ripeness sensor

7. PRELIMINARY TESTS USING THE PROTOTYPE

This section summarizes results obtained using the prototype described in section 6. The prototype uses only the single pulse technique and a simple peak detector. The detected signal represents only the magnitude of the decaying resonance signal induced by the magnetized sample in the detect coil. In the IRFT experiments (section 4) and the in-tact fruit tests (section 5), sequences of pulses were applied to the sample. Those types of experiments are not possible on the first generation prototype. However, equipment on order from the Southwest Research Institute in San Antonio Texas includes a quadrature detector. It will also interface with a pulse programmer. Therefore, the second generation prototype will be capable of experiments which employ different pulse sequences. This will allow us to identify the best techniques for detecting sugar content in intact fruit. We will also be able to experiment with methods of analyzing the signals to achieve the maximum sensitivity to differences in sugar content in the shortest possible time interval.

In the first generation prototype, an alternating magnetic field of about 0.8 gauss was generated in the RF/detect coil and the pulse width was $80~\mu sec$. Output signals were accumulated 6 to 10 times. Different output signal sensitivities can be achieved by adjusting the capacitors in the tuning circuit. The sensitivity is a maximum at an exact resonance point. However, from a practical standpoint, it is difficult to find this point. Nevertheless, good sensitivity can be achieved at a point close to the resonance point. The phase of resonance signals differs by 180° when the point is approached from opposite directions. The sensitivity changes whenever the probe is tuned.

7.1 Analysis of the Signal

The output signal is derived from the FID resonance signal and is also affected by three factors: inductance of the probe coil, damping coming from the circuits, and magnetic field homogeneity. When the magnetic field homogeneity is increased, the decay time of the resonance signal increases along with the signal sensitivity. We investigated the effect of the *inductance change of the probe coil caused by insertion of different samples in the coil* (This is related to the dielectric properties of the sample). By tuning the circuits, we can vary the relative effects of the inductance change of the probe coil and the resonance signal. There are three possible situations:

- [1] We can tune circuits so that the output signals are mainly affected by the inductance change of the probe coil when different samples are inserted. In this case, the output signals are just shifted in parallel.
- [2] We can tune the circuits so that the output signals are mainly affected by the FID resonance signal coming from the samples. In this case, there is almost no shift, and the maximum values and slopes respond to the differences in sugar content. The peak height is a measure of the initial amplitude of the FID resonance signals and the slope is related to the decay time of the resonance signals. This is the desired result because the sample inductance does not affect the signal.
- [3] We can tune the circuit so that the output signals are affected by both the inductance change and the resonance signal. Even though case [2] is, theoretically, the most desirable, with our circuit,

Ripeness Sensor Dev. Preliminary Test

we achieve a higher signal sensitivity with this method. According to our experience, the optimum combination for the resonance signal is to have about 80% from the resonance effect and about 20% from the inductance change.

7.2 Test of Sugar Solutions

Two samples were used for the initial test: glycerin and water. The signal outputs from the two samples were accumulated 6 times and averaged. They are plotted in Figure 17. Glycerin is very sticky and has a high viscosity. It has a shorter FID decay time (i.e. higher slope) than water. By tuning the sample coil carefully and changing the pulse width and power, good sensitivity can be achieved. In repeated tests over a period of three days, the signal from the glycerin sample had a shorter T_2 time (i.e. higher slope) than the water sample. This is as expected.

After the initial tests, we improved the sensitivity of output signals by matching impedances. We also discovered that we were not capturing the entire peak because there was a delay between the trigger and receive modes. We solved this problem by rewriting the computer software. This also improved the sensitivity of the signal. Five different sugar solutions have been tested: water (0% sugar), 2%, 9%, 15%, and 42% sugar-water mixtures. Plots of the output signals are shown in Figure 18. The initial peak height, 50th data point (at 2.5 msec) and 80th avg. ([70th data point + 90th data point]/2) were determined and labeled MAX, 50th, 80th.av, respectively. The peak heights are proportional to the total number of protons in the samples and the slope is related to the decay time of the resonance signals coming from the samples. The signal from 2% sugar was almost identical to the water signal. We can currently separate solutions differing in sugar content by 4% or more.

7.3 Test of Intact Fruit

The probe we are currently using for the liquid samples has a relatively large sample coil (about 2.5 in long and 1 in diameter). This makes the coil much longer than the diameter of fruits such as grapes (about 0.75 in) and blueberries (about 0.5 in). In thess tests, the fruits are placed in a test tube (0.75 in inside diameter) of the same size as the test tube used for testing the sugar solutions. This means that the filling factor is poor -- the volume of a single grape is too small (compared to the volume of coil) to give a sufficiently strong signal. We measured the sugar contents of red and white grapes (10 each) using a refractometer. The sugar contents of red grapes varied from 15 to 18% and the white grapes varied from 16 to 22% sugar. The signal sensitivity from the semi-solid samples decreases as compared to the liquid sugar solutions. Therefore, the sugar content of the grapes does not vary sufficiently to allow the probe, with its current level of sensitivity, to detect differences. However, we were still able to conduct a test of the effect of the grape sugar content by artificially increasing the filling factor and injecting a sugar solution into a grape as described below.

When we placed four grapes in a test tube (0.75 in inside diameter) and lowered them into the probe (1 in inside diameter), we recorded the signal marked "A" in Figure 19. After adding a fifth grape, we obtained the signal marked "B." We removed the fifth grape, injected it with 40% sugar solution using a syringe, allowed the grape to stand for 30 minutes, placed the grape on top of the other four grapes in the test tube, and returned the test tube to the probe. The signal produced is designated by "C" in Figure 19. The injection of the sugar solution increased the sugar content by about 8%.

Two banana samples were also tested: green and yellow. Core samples were inserted into the 0.75 in sample tube. The signal outputs are shown in Figure 20. The green banana had 9.2% sugar and the yellow one had 15.4% sugar. The sugar content of grapes was artificially increased by soaking them in

Ripeness Sensor Dev.
Preliminary Test

40% sugar solution for one week. Two grapes were tested individually: one soaked and one not-soaked. The soaked grape contained 23.8% sugar and the other had 17.6% sugar. The output signals are shown in Figure 21.

7.4 Conclusions

The peak height of the output signals is related to the number of protons in the samples. The slope corresponds to the decay time of the resonance signals. Other factors which affect the output signals include the inductance change of the detect coil, damping of circuits, and magnetic field homogeneity. Elimination of these effects will increase the sensitivity. With the current probe, output signals of sugar solutions differing by about 4% (or more) in sugar content can be separated. However, for grapes and bananas, output signals can be separated when differences in sugar content are about 6% (or more). The sensitivity is lower for individual fruits as compared to the liquid sugar solutions, because they are semisolid.

References

- [1] Rollwitz, W.L. 1985. Using radiofrequency spectroscopy in agricultural applications. Agricultural Engineering, 66(5):12-14.
- [2] Minispec application note. 1990. Bruker Analytische Messtechnik GmbH, West Germany.
- [3] Rutar, V., M. Kovac and G. Lahajnar. 1988. Improved NMR spectra of liquid components in heterogeneous samples. J. Magn. Reson., 80:133-138.

Figures

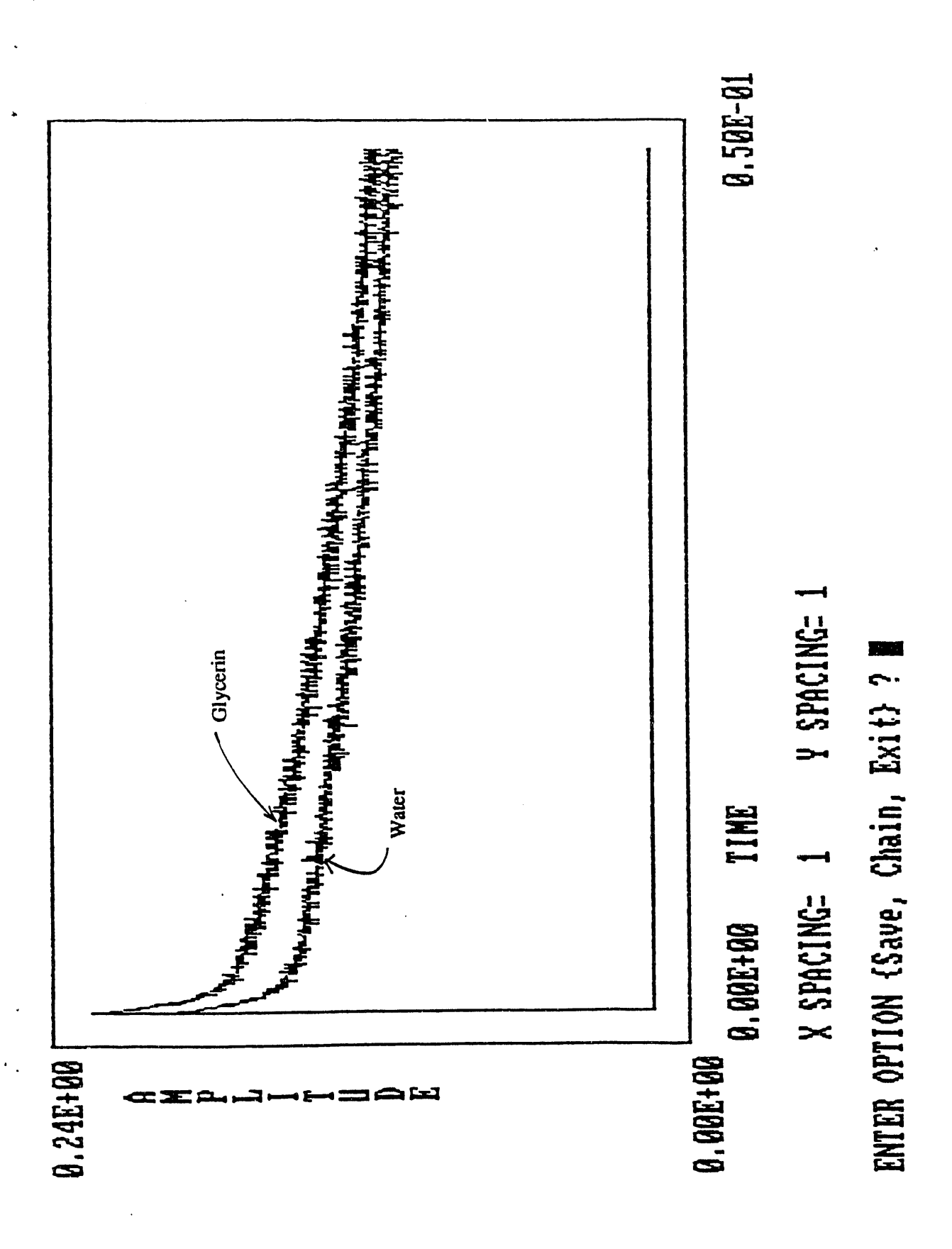


Figure 17. Output signals from glycerin and water samples

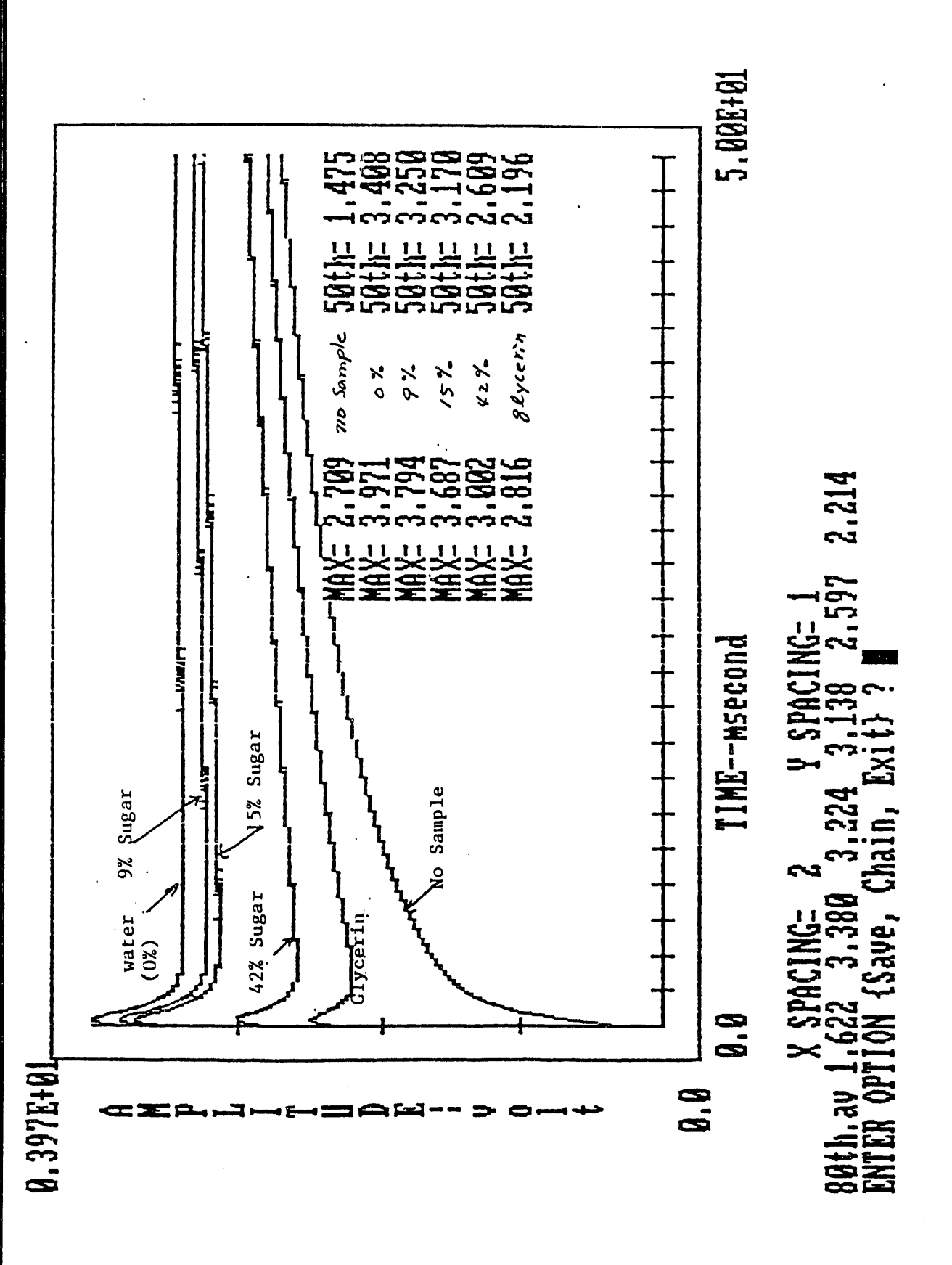


Figure 18. Output signals from different sugar solution samples. The phase of the resonance signals is shifted by -180° compared to the signals in Figure 17.

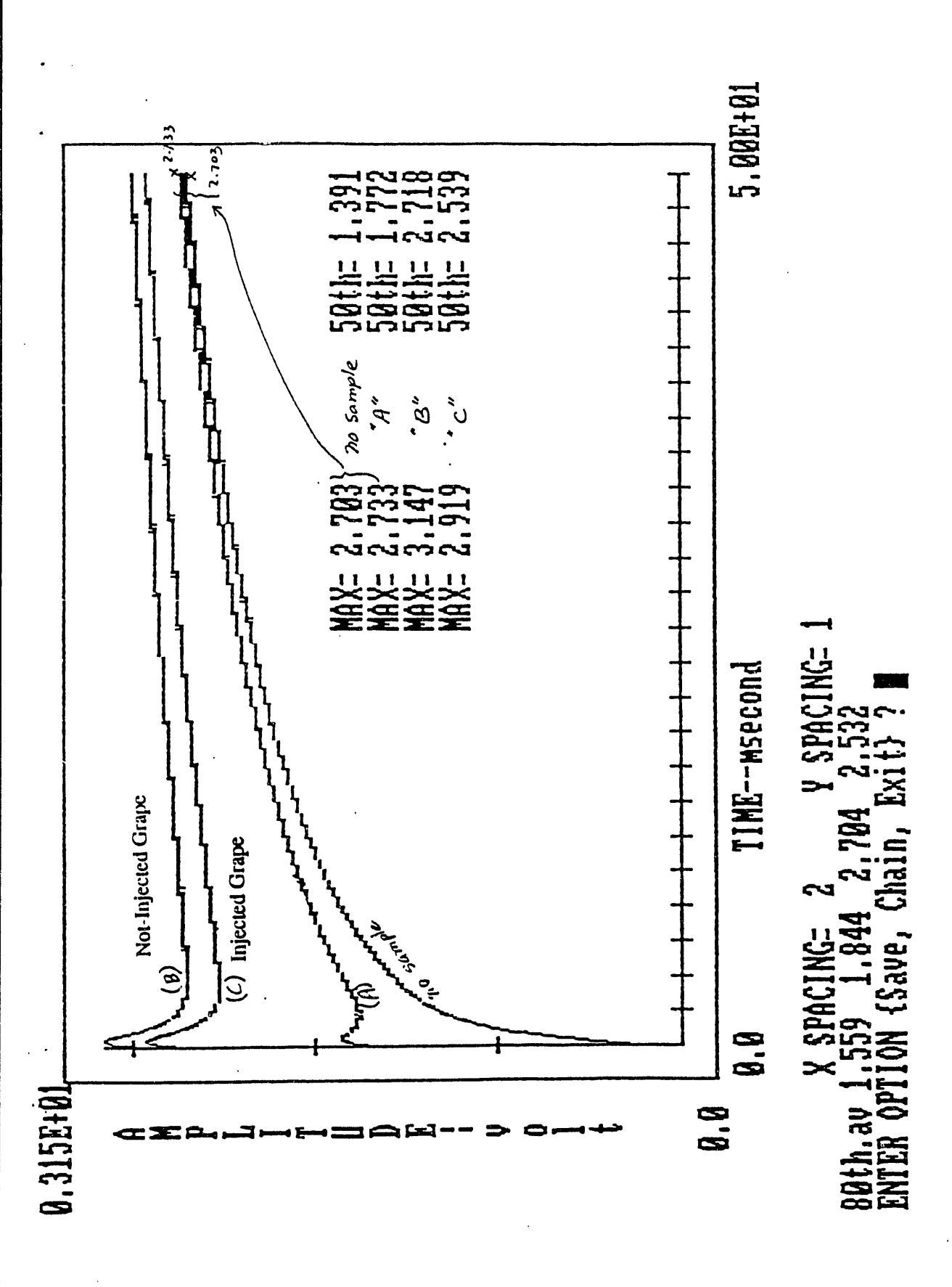


Figure 19. Output signals from individual grapes. The phase of the resonance signals is shifted by -180° compared to the signals in Figure 17.

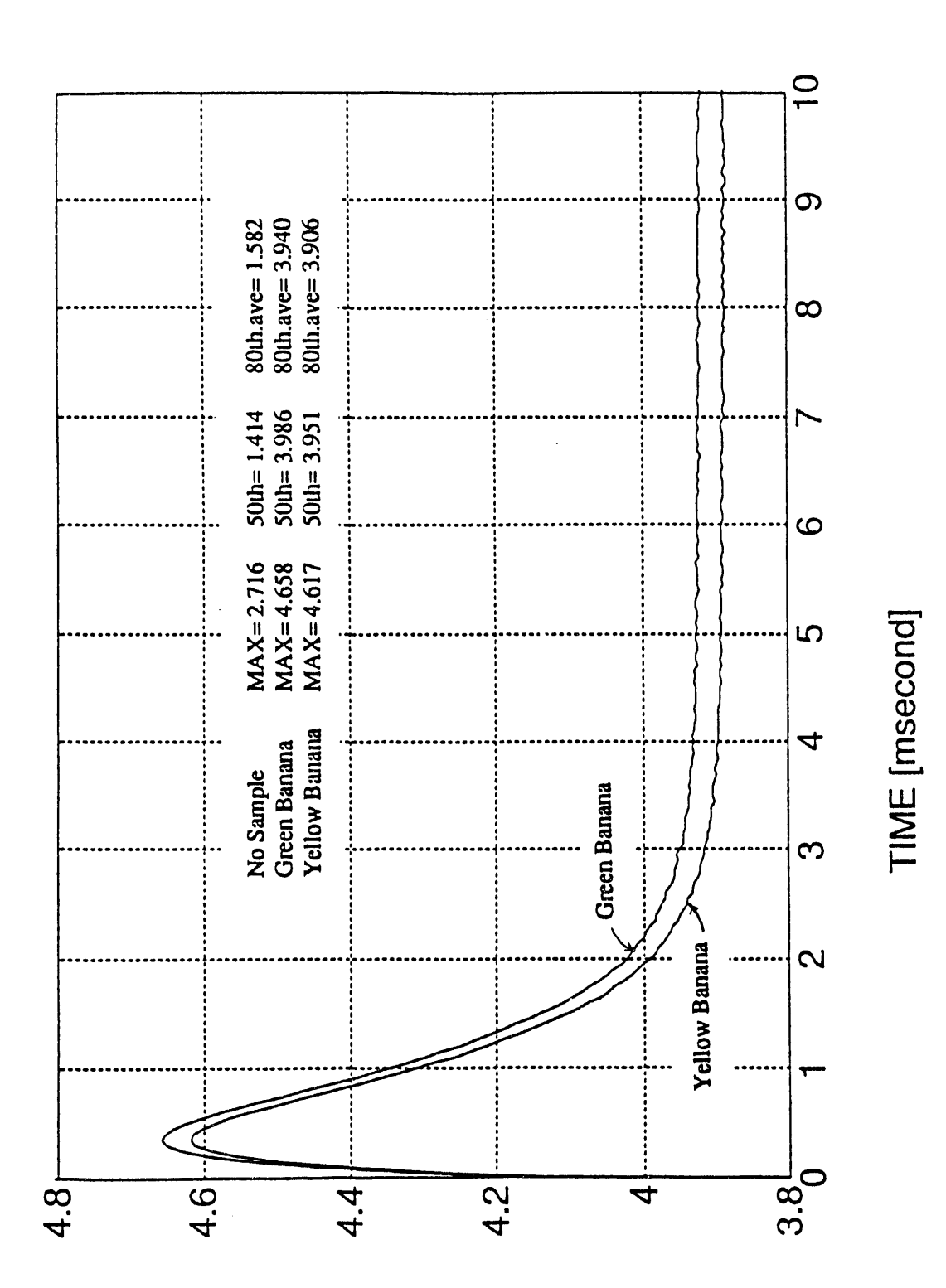


Figure 20. Output signal from green and yellow bananas. The phase of the resonance signals is shifted by -180° compared to the signals in Figure 17.

AMPLITUDE [volt]

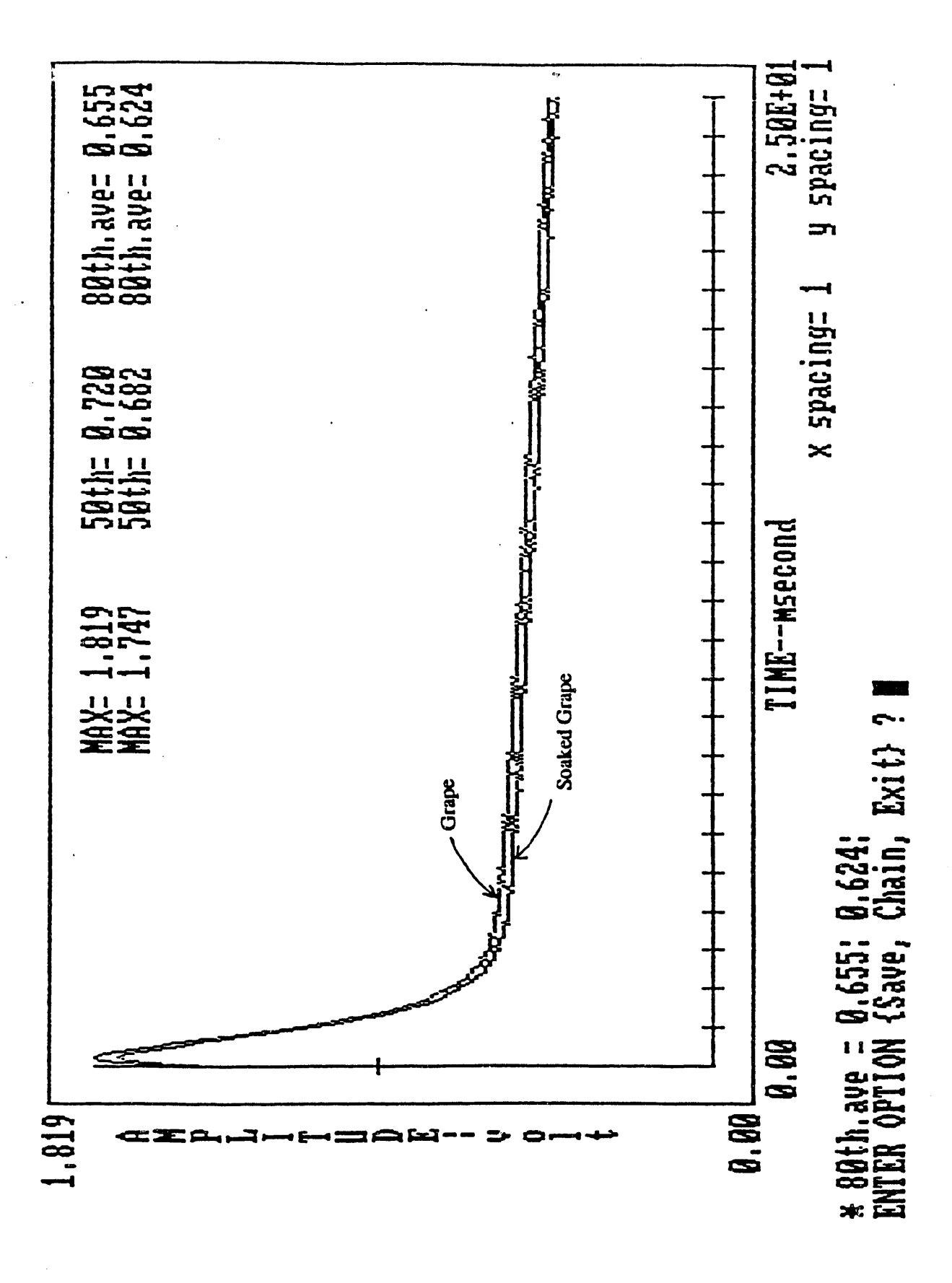


Figure 21. Output signal from individual grapes. The phase of the resonance signals is shifted by -180° compared to the signals in Figure 17.

SUMMARY

This study investigated the feasibility of utilizing proton magnetic resonance (1 H-MR) for determination of fruit ripeness. The proposed sensor would rapidly and nondestructively measure sugar content of individual fruits and vegetables with an accuracy of $\pm 1\%$. Since the sugar content of most fruits and some vegetables changes during the ripening process, sugar content would be used as an indicator of ripeness. Grocery stores and consumers must discard a significant proportion of the fruits and vegetables which they sell/utilize. A review of the literature combined with a telephone survey of groceries and wholesalers revealed that nondestructive ripeness sensing could save approximately 4 to 7% of the annual U.S. production (39 million tons) of the 17 major fruits and vegetables. When fruit is discarded, the energy used in producing, transporting, and storing the fruit is also lost. When the 4 to 7% savings is applied to the 39 million ton annual U.S. fruit production and combined with potential savings of energy for storage of the remainder of the crop, the result is an estimated annual energy savings of 24 x 10^{12} BTU's.

Proton magnetic resonance instruments are based on the interaction of protons (hydrogen nuclei) in samples with two perpendicular magnetic fields. Samples are placed within a strong magnetic field (B₀) which is procuced by either permanent magnets, electromagnets or superconducting magnets. Protons associated with sugar and water molecules in the sample align with the magnetic field. The protons' predisposition towards orientation within the B₀ magnetic field is further exploited by another relatively small magnetic field (B₁). The B₁ field is generated by sending a radio frequency (RF) pulse through a coil surrounding the sample. The transient B_1 magnetic field is at right angles to the B_0 magnetic field. The frequency of the RF field in relation to the strength of the B₀ magnetic field determines which molecular units are affected. When the RF pulse is finished, the transient field dissipates rapidly and the protons return to their original orientation. The rate of reorientation is dependent on the particular molecule with which the proton is associated and occurs more rapidly for the protons in the water than for the protons in the sugar. The reorientation induces a very small alternating current signal in a receiving coil (which can be the same coil used to generate the transient field). This signal can be amplified and viewed on an oscilloscope or captured by a computer and further analyzed. The amplitude of the signal decreases with time in a process called *free induction decay* (FID). The FID rate of the protons depends on the type of molecule with which they are associated. A proton (hydrogen nucleus) associated with water has a decay rate different from that of a proton associated with sugar. The rate at which the decay occurs can be quantified by a numerical value called the time constant, T₂. It is an approximate measure of the time required for the amplitude of the FID signal to decrease to one third of its original value.

An alternative method of analyzing the signal applies a fourier transform (FT) to the output signal. The FID signals from protons associated with different molecules have different frequencies. The frequency of the signal produced by the protons in water differs from the signal frequency of protons in sugar. When the FT is applied, the signals from the two types of protons appear as peaks located at different frequencies. In general, the stronger the permanent magnetic field, the better the resolution of the signal into peaks. High resolution devices usually use very strong superconducting magnets with field strengths in the order of 40 to 80 kilogauss. The radio frequency used to create the transient magnetic field is related to the strength of the magnetic field by the magnetogyric constant, which is 0.004258

MHz/gauss for hydrogen detectors. A ¹H-MR detector operating at an RF of 200 MHz uses a superconducting magnet with a field strength of 47 kilogauss.

The investigator is not limited to measuring T_2^* of the FID signal. When the transient field is applied and then removed, the original magnetization of the sample is perturbed but it then returns to its original value. The time constant which characterizes the rate at which the original magnetization returns is called the *spin-lattice relaxation time*, T_1 . There are several techniques that can be used to measure T_1 including the Inversion Recovery Fourier Transform (IRFT) technique. In the IRFT technique a pulse is used to invert the magnetization of the sample (reverse its direction). After a predetermined time interval, during which the original magnetization begins to recover, a second pulse is applied in such a manner that it produces a signal in the receiving coil. Embedded in the signal are several frequencies which are associated with the protons in water and the several types of sugar. These frequencies are determined by applying a fourier transformation to the signal.

The measurement of the decay of the free induction signal described above was only approximate. There are alternative methods which allow determination of the true value, T_2 , called the *spin-spin relaxation time*. The error in measuring T_2 is in part caused by slight inhomogeneities in the magnetic fields (B_0 and B_1). In samples which are mixtures of solids and liquids, the magnetic properties of the sample are not homogeneous. This introduces additional magnetic field inhomogeneities. In the Carr-Purcell-Meiboom-Gill procedure, a sequence of RF pulses are supplied to the coil in such a manner that the effects of the inhomogeneities are eliminated. When several nuclei are present, the values of T_2^{\bullet} and T_2 may differ significantly. This obscures information that can be obtained from the signal. Therefore, more information can often be obtained by measuring T_2 values.

The concept of measuring sugar content by means of proton magnetic resonance was first tested using water-sucrose solutions and core samples 5 mm in diameter taken from bananas and apples. These tests were conducted with high resolution magnetic resonance equipment (200 MHz) such as that used by chemists and pharmacists for precise determinations of chemical composition or chemical bonding. The relatively simple single pulse technique was utilized. In samples consisting of sugar dissolved in water, the protons in the sugar and water molecules gave peaks which were relatively close together, yet distinct. For samples containing 2 to 15% sucrose by weight, the height of the sugar peak was linearly correlated with the percent sugar in the solution.

In the next series of experiments samples were taken from intact fruit, where water is associated with other molecules and is influenced by cell structures, and where several simple sugars are dissolved or partially dissolved in the cell water. The fourier transformation was applied so that separate peaks were obtained for the protons in the sugar and the water. When apple and banana samples were tested, the water peak predominated and the sugar peak (which was a composite of several similar peaks arising from the various types of sugar found in the fruit) appeared as a relatively small, yet distinct, *bump* on the descending portion of the water peak. In these tests, the sugar peak of a green banana, which contained 8% sugar, could not be detected. However, over the normal range for moderately ripe to very ripe bananas, 15 to 23% sugar, there was a linear correlation between sugar content and height of the sugar peak (r=0.94). In the case of apples, the sugar content ranged from 11.5 to 15% and was also linearly correlated (r=0.87) with sugar peak height.

The experiments with bananas suggested that the single pulse technique could not be used for samples low in sugar content (e.g. below 10%). Therefore, several more sophisticated techniques were examined. The IRFT sequence, mentioned above, was the most promising. The technique has the advantage of being able to suppress the peak caused by the protons in the water molecules. This suppression is achieved by careful adjustment of the length of the pulses and the delay time between the first and second pulse. Sugar peaks could be detected for samples of cantaloupe containing as little as

1.8% sugar. Over the range of 1.8 to 13% sugar, the peak height was related to the sugar content. The relationship was better described by a second degree polynomial (r=0.98) than by a linear correlation (r=0.94). The IRFT technique requires slightly less than 2 seconds for a sample determination. However, if accuracy can be sacrificed slightly so that measurements are made to $\pm 1\%$, then it may be possible to reduce to milliseconds the time required for a sample measurement. There are other methods of analyzing the signal from the single pulse technique which can be evaluated. These may give resolution at sugar contents as low as 2% with and accuracy of $\pm 0.5\%$.

Following validation of the concept using high resolution devices, test were conducted with a low resolution device. These experiments were important because the proposed sensor is of the low resolution type. Use of the smaller magnet has practical advantages because it makes the device more portable and lowers the cost. Cherries and grapes were tested in a 10 MHz proton spectrometer sold commercially for use in the food and chemical industries. The magnet used in the device has a field strength of approximately 2,350 gauss. This is relatively small in relation to the field strength of the high resolution devices used for testing the core samples. There was a wider air gap between the magnets of this instrument and this allowed use of a larger sample. The test tube used to hold the samples had an inside diameter of 24.5 mm and could accommodate intact grapes and small cherries. The spectrometer utilized the CPMG technique for determinations of T_2 of the protons in the water in the grapes and cherries. There was a significant linear correlation between the time constant and the sugar contents of the grapes and cherries (r=0.66 for grapes; r=0.62 for cherries). It should be possible to improve this correlation by using a measurement technique which suppresses the water resonance. As a result, the time constant would be affected mainly by the protons in the sugar.

The cherries evaluated in the tests described above varied widely in firmness. Such variations are produced by wet weather when the cherries are ripening and by bruising during handling. The firmness of the cherries was measured by compression tests conducted immediately following the proton magnetic resonance tests. Firmness was linearly correlated (r=0.6 to 0.7) with T_2 of the CPMG signal. Recall that the protons in the water had the dominant influence on the signal. Firmness is related to sugar content (and probably also water content) in undamaged fruit. Riper fruits are softer. However, damage to tissues would cause changes in the state of water and sugar in the fruit. It may be possible to detect these types of changes by means of an additional measurement of T_1 or by applying other pulse sequences such as IR (inverse recovery). It would then be possible to use low resolution magnetic resonance to evaluate both sugar content and firmness.

The final step in the evaluation process was the development of a prototype. A magnet console was designed using an interactive graphics simulation of a finite element model. This gave a design which had a homogeneous magnetic field of the desired strength. RF transmitting and receiving circuits were built which allowed the magnet console to be used for detecting the first several undulations in the free induction decay curve. A single pulse technique was used for a first generation prototype. Although this circuitry was relatively simple, it made possible a preliminary evaluation of the technique and the console. The prototype accommodates samples with a diameter less than or equal to 19 mm. Samples tested in the prototype included sugar solutions of varying concentration, core samples of banana, and whole grapes. The grapes were relatively uniform in sugar content. Therefore, the sugar content of several grapes was increased by soaking them in a sugar solution.

The shape of the output signal varied with the sugar content of the sample. This variation could be quantified by comparing the maximum height of the peaks and the height of the curve (the voltage) at two additional times. The curves for sugar water solutions varying by 4% or more in sugar content could be distinguished. In the case of banana samples and grapes, curves could be distinguished for sugar content differences of 6%.

Ripeness Sensor Dev. Summary

The circuitry of the prototype was relatively simple. A single pulse was used. Only the first portion of the FID signal was detected. However, the protons in sugar have a greater effect on the first portion of the FID curve. Use of the simple circuit precluded more sophisticated techniques such as fourier transformation (FT) of the signal. Recall that FT is capable of resolving the signals from the sugar and water protons into two distinct peaks. More sophisticated equiment arrived on June 28. It was built by the Southwest Research Institute in San Antonio Texas which has had 20 years of experience with low resolution magnetic resonance and has spent many years designing and testing magnetic resonance equipment. The equipment will be used for phase II of the project. It will give a stronger signal and a much better FID signal. A pulse programmer, currently being built by the phase II industrial partner, Magnetic Instruments, will be connected to the equipment so that sequences of pulses can be utilized. This will allow many additional experiments including a more thorough evaluation of techniques for improving the sensitivity of the signal to sugar protons. It should also permit a reduction in the time required to make individual measurements.

RECOMMENDATIONS

Although preliminary results were quite promising, further evaluations of ¹H-MR sensing of fruit ripeness are needed. The tests with existing laboratory devices confirmed that the technique can be used for ripeness sensing and defined test procedures, such as water peak suppression by the IRFT method, which could be used to improve sensitivity in low resolution devices.

However, additional laboratory tests are needed (a) to determine which parameters $(T_2^*, T_2, \text{ or } T_1)$ are best correlated with sugar content and firmness, (b) to identify the best method(s) of measuring these parameters (e.g. delay times between pulses, pulse lengths, and number of signals which must be averaged), and (c) to develop alternative methods of analyzing signals (e.g. height, area or shape of the FID signal). Tasks (b) and (c) require an extensive and precise evaluation of the RF signals produced by the fruit samples. This evaluation would be facilitated by use of a spectrum analyzer. This device can detect the signals for accurately and can determine their frequency components and the amplitudes of these components. It can also measure noise and distortion.

Studies should also be conducted on fruits and vegetables to identify changes in water content, sugar content, and composition during the ripening process. The analyses will include chromatograph tests to determine the kinds and amounts of various simple sugars present in the fruit. (Note: There are slight variations in the magnetic resonance response of these various simple sugars.) Changes in cell structure (e.g. membrane permeability, state of water, location and form of sugar) should be identified. This information will give insight into pulse sequences and signal analysis techniques which will be most successful in distinguishing differences in ripeness and firmness.

Modifications to the prototype are also needed. The circuitry of the prototype tester and the probe design should be evaluated and modified so that the signal to noise ratio is improved. This would be facilitated by use of a vector impedance meter which can be used for impedance matching and proper tuning. The probe can be built with magnets made of any of several types of materials: aluminum-nickel-cobalt, rare earth, or neodinium boride. The aluminum-nickel-cobalt is less expensive and is less sensitive to temperature variations. The neodinium boride magnets produce a stronger magnetic field for a given weight of material and the field is more homogeneous. However, these magnets are relatively expensive. The rare earth magnets have intermediate properties. The relative advantages and disadvantages of each of these materials should be evaluated using prototypes. In addition, a mechanism must be developed which will accurately and rapidly position the sample within the coil.

DATE FILMED 21/6/193

	•	T)	4.11
	•		
	•		
	•		
•			